Interfaces and Free Boundaries **19** (2017), 417–447
DOI 10.4171/IFB/388

Hysteresis in porous media: Modelling and analysis

BEN SCHWEIZER
Technische Universität Dortmund, Fakultät für Mathematik,
Vogelpothsweg 87, 44227 Dortmund, Germany
E-mail: ben.schweizer@tu-dortmund.de

[Received 2 September 2016]

Unsaturated flow through porous media can be modelled by a partial differential equation using saturation s and pressure p as unknowns. Experimental data as well as elementary physical arguments show that the coupling of the two variables must take into account hysteresis. In this survey, we describe the physical origins of porous media hysteresis, present the ideas of its mathematical description, and review the analysis of the resulting hysteresis models.

2010 Mathematics Subject Classification: Primary 76S05; Secondary 47J40, 35K55.

Keywords: Porous media, hysteresis, unsaturated flow, gravity fingering.

1. Introduction

The quantitative modelling of groundwater flow is a young field – compared to the modelling of heat or electric conduction. It has its foundations in the work of Darcy of 1856, but partial differential equations for its description appear as late as 1931, formulated by Richards in [79]. Richards identified saturation and pressure as the two fundamental variables for the description of porous media. He formulated the law of capillary pressure and combined it with mass conservation and Darcy's law. Additionally, he described how the "water retention curves" (capillary pressure curves) can be measured, and observed that hysteresis is important in the system: After a description of experimental data, Richards writes in [79]:

> It is apparent for a 4 mm layer of soil in a rather loose state of packing there is a considerable hysteresis effect over the pressure range studied.

The development of a model for the hysteresis effect took some time. In the year 1954, Everett and Smith described a first model in [27] as follows:

> [...] a system exhibiting hysteresis can be treated, at least formally, as an assembly of independent domains. Each domain is supposed to exist either in state I or in state II, conversion from one to the other being brought about by a change in the external variable x.

The idea that hysteresis can be modelled as a collection of switches had tremendeous impact, and the name *domain theory* has been used since then. The (independent) domain theory assumes that the system is a collection of independent switches (= domains = relays); here the external variable is the pressure, $x \cong p$. We emphasize that the following names really describe the same idea:

$$\text{domain model} = \text{assembly of independent switches} = \text{Preisach model}$$

We want to outline the theory and its mathematical description in this overview.

In the engineering community, the name "domain" is used, mathematicians prefer the name "Relay". We take the different names as a method to distinguish different points of view: In Section 3 we discuss the more applied developments under the name "domain models". In Section 4 we discuss the mathematical developments using the names "Relay" and "Preisach model".

Outline of this survey. Section 1.1 of this introduction contains some remarks on hysteresis in general. In Section 1.2 we discuss the modelling of porous media and, in particular, the arguments leading to the assumption of a capillary pressure relation (coupling pressure p and saturation s). The analysis of the resulting porous media models (without hysteresis) is sketched in Section 1.3.

Section 2 is devoted to the effect of hysteresis in the p-s-relation: We describe experimental methods to measure the relation and sketch the qualitative outcome, which exhibits hysteresis. We illustrate the three fundamental mechanisms behind the effect: velocity dependent contact angle, bottle-neck effect, snap-off effect. We also mention some phenomenological models.

Section 3 is devoted to the development of the domain model for hysteresis. We discuss the influencial contributions of Everett, Enderby, Poulovassillis, Philip, Mualem and others. Essentially, in these models, the pressure p is regarded as a macroscopic quantity that triggers each of the switches (each of the domains) simultaneously. The local water content is 0 or 1 in every switch and the saturation s is an average over all the switches. We review the development of this theory and its practical applications.

Section 4 is concerned with the mathematical analysis of hysteresis models. We start from the elementary switch-type models (hysterons) and indicate how generalized models are obtained by a superposition of hysterons. We review mathematical results for these models.

Section 5 is devoted to combinations with rate-dependent effects and other extensions. In particular, we discuss the effect of gravity fingering. This effect is important for us, since it can only be explained with hysteresis equations. In this sense, gravity fingering is a test-case for hysteresis models.

Let us mention here two recent overview articles. The survey [1] discusses hysteresis mechanisms and models. In comparison to that survey, we discuss the subject from a more analytical perspective. The overview [103] is more general, it is concerned with the mathematical treatment of partial differential equations with hysteresis and not focussed on porous media.

1.1 *The phenomenon of hysteresis*

The word "hysteresis" is ancient Greek for "to lag behind" and expresses nicely an important qualitative property of a system with hysteresis. Consider the classical hysteresis loop of Figure 1 (left), where the dependence of an output w on an input u is sketched. When u increases, also w increases, when u decreases, also w decreases. But after the reversal of the input direction, the pair (u, w) does not follow the original path. The output is not in an algebraic relation $w = F(u)$ with the input. Instead, w lags behind u: For an increasing input u, the values of the output w are somehow "too small", while for a decreasing u, the values of w are "too large". We observe that the values of w depend not only on the current value of u, but also on the history of the process *(memory effect)*.

Let us describe here briefly two other important hysteresis phenomena: Ferromagnetism and plasticity. For overviews, also on the history of hysteresis modelling, we refer to [11, 98].

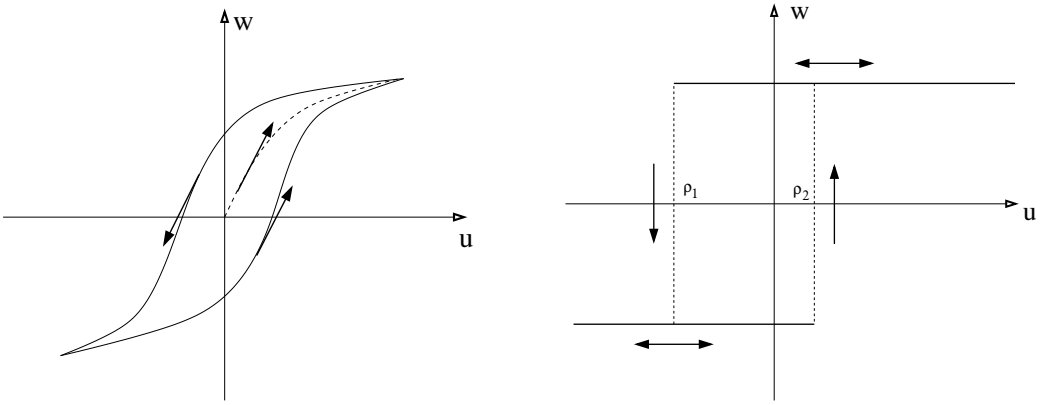

FIG. 1. Left: A hysteresis loop. An increasing input u results in an increasing output w, and a decreasing u results in a decreasing w. But the changes of w lag behind those of u. Right: The Relay hysteron, a switch with delay. The Relay shares qualitative properties with the hysteresis loop. It can be used as a building block for more complex hysteresis effects.

Ferromagnetism. Among the best know hysteresis effects is that of magnetism: When a ferromagnet (e.g., iron) is exposed to a magnetic field with strength $u \cong H$, the magnetization $w \cong M$ of the sample shows the behavior of the loop in Figure 1 (left). The effect was already well-known in the 19th century and Lord Rayleigh proposed in 1887 a first model (in modern terminology: a Prandtl–Ishlinskiĭ model of Play type, see Section 4.2). More influential was the model of Preisach from 1935 [77], since he could complement his model with a geometrical interpretation (the Preisach plane, see Section 4.1).

Plasticity. The other famous example for hysteresis is the plastic deformation of metals: Applying a force (stress) $u \cong \sigma$, the sample responds with a deformation (strain) $w \cong \varepsilon$. Deforming the sample (moving it to the top right point of the hysteresis loop) and then releasing the force (moving along the loop back to $u = 0$), the material remains deformed ($w > 0$). We remark that the hysteresis loop for plastic deformations looks quite different from that of Figure 1, but qualitative features are shared.

While plastic behavior has certainly been observed since thousands of years, the quantitative description of plastic hysteresis started in the 19th century with Tresca (maximum shear stress yield criterion in 1864) and Saint Vénant (perfect plasticity in 1870). Later, von Mises introduced multi-dimensional yield-criteria (1913) and Prandtl formulated a model using Stop-hysterons and their superposition (1924 and 1928). Due to his fundamental contributions and the parallel invention by the Russian mathematician Ishlinskiĭ, the model is today called the Prandtl–Ishlinskiĭ model. We describe it in Section 4.2.

1.2 *Fundamentals of porous media modelling*

For the rest of this introduction, we are not concerned with hysteresis, but only with the modelling of porous media (without hysteresis).

The essence of most models for flow in porous media is to describe the state of the medium (in every point x in space and at any time t) by two variables: $s = s(x, t)$ stands for the saturation in

the medium, $p = p(x,t)$ for the fluid pressure in the medium. The saturation s is related to the mass of fluid per volume; it is a macroscopic variable in the sense that it denotes an average over many pores. One usually defines s to be the fraction of pore space that is occupied by water; in this way, s takes values between 0 (no water) and 1 (complete saturation). To calculate the proportion of fluid volume in the medium, one has to make use of the porosity ϕ (pore volume per unit volume): At saturation s, the fluid occupies the percentage ϕs of the volume. Conservation of mass takes the form $\partial_t(\phi s) + \nabla \cdot F = 0$ for some flux function F. We will suppress the constant ϕ in the following and set it equal to 1 (which can be done by normalizing the flux function).

To describe the flux function F one uses Darcy's law: The pressure p generates locally the force $-\nabla p$. Combined with the gravity force g, the driving force for a fluid particle is $-\nabla p + g$. Darcy's law assumes that the flux F is proportional to the force field in the porous medium, with a proportionality factor $k = k(s)$ that depends on the saturation s, hence $F = k(s)[-\nabla p + g]$. Here, $k : [0,1] \to [0,\infty)$ is a non-negative and bounded coefficient function, usually monotonically increasing. We remark that, in applications, the function k depends also on the spatial position x.

The combination of mass conservation and Darcy's law leads to the porous media model

$$\partial_t s = \nabla \cdot \big(k(s)[\nabla p - g]\big)\,, \tag{1.1}$$

which must be complemented by some relation between p and s.

When the porous medium occupies a domain $\Omega \subset \mathbb{R}^n$ and processes occur on a time interval $(0,T)$, the problem is to find two fields $s : \Omega_T \to \mathbb{R}$ and $p : \Omega_T \to \mathbb{R}$ that solve (1.1) on the space-time domain $\Omega_T := \Omega \times (0,T)$. The diffusion coefficient $k = k(.)$ and the gravity force g are given. An initial condition for s and boundary conditions for p along $\partial\Omega \times (0,T)$ must be prescribed.

Equation (1.1) expresses mass conservation, using Darcy's law for the flux. It is widely accepted as an accurate model for unsaturated single-phase flow. Hysteresis in porous media concerns the relation between p and s. Below, we will briefly describe the arguments that lead to the capillary pressure assumption $p = \Phi(s)$, the model without hysteresis. We emphasize that this law does not express a physical principle and that we will modify it later on in order to take hysteresis effects into account.

The capillary pressure function. In order to close the system (1.1), the simplest choice is to assume that p is in a monotone algebraic relation with s,

$$p = \Phi(s)\,. \tag{1.2}$$

By this relation we mean the pointwise dependence $p(x,t) = \Phi(s(x,t))$ for a strictly monotone function $\Phi : [0,1] \to \mathbb{R}$. The latter may also be assumed to be x-dependent. It is often denoted as $p = p_c(s)$ for "capillary pressure".

Essentially, the argument for (1.2) is as follows: Let us consider a hydrophillic medium which is in contact with water. When some pores of the medium are partially filled with water, there are interfaces between water and air in these pores (compare Figure 2). These interfaces are curved due to contact angle conditions. Surface tension generates a pressure difference in the two fluids. When we assume that air has the constant pressure 0, then the pressure of the water is negative (capillary pressure).

This negative pressure is the cause of the absorption of water by a hydrophillic material: Negative water pressure at the interfaces (menisci) leads to a pressure gradient in the pore channels.

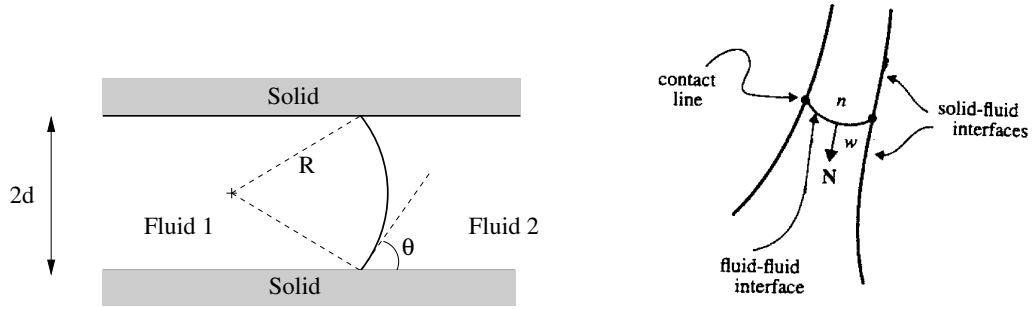

FIG. 2. The origin of capillary pressure. Left: A fluid-fluid interface in an idealized pore. The width $2d$ of the pore together with the contact angle condition determine the curvature $1/R$ of the meniscus. Right, from [35]: A change in the position of the interface results in a change of the capillary pressure, since the pore diameter changes.

In the absence of other forces, the result is a water flow from the reservoir towards the menisci. This leads to an advancement of the interfaces and an increasing saturation in the specimen.

The capillary pressure is high in absolute value when the interfaces are located in small pores. When much water is contained in the medium (the value s is large), then the small pores are already filled and only large pores suck in water. In large pores, the curvature of menisci is small, hence the pressure is small (in absolute value). We conclude that the pressure difference decreases when s increases. With this argument, the capillary pressure (which coincides with the water pressure p if the air pressure is set to zero) can be regarded as a function of the saturation, $p = \Phi(s)$ as stated in (1.2).

Notation in the literature.. The pressure function p (or its absolute value $|p|$) is often denoted as Ψ. It is helpful to keep in mind how a pressure can be measured: If a (hydrophillic) porous medium is in contact with a water basin, then the suction of the porous medium leads to a (partially) wetted medium even if the medium is above the water level of the basin (compare Figure 3, right). The difference in height is the "suction". The suction is proportional to the capillary pressure. The saturation s is often called "water content" and denoted with the symbol θ. With the inverse $\Theta := \Phi^{-1}$, the capillary pressure relation can also be written as $s = \Theta(p)$.

The Richards model is widely used and many analytical results are available, but we must recall that the relation $p \in \Phi(s)$ is phenomenological: Not even in a crude approximation, a porous medium can be constructed as a collection of straight tubes, since the tubes must have junctions to form a connected pore space. And, in fact, the capillary pressure law does not give a correct description: It does not include hysteresis, and hysteresis is an experimental fact.

1.3 *Analysis of porous media models without hysteresis*

Inserting the pressure-saturation relation (1.2) into (1.1), we obtain the Richards equation

$$\partial_t s = \nabla \cdot \Big(k(s) \big[\nabla \big(\Phi(s) \big) - g \big] \Big) . \tag{1.3}$$

Due to non-negativity of k and monotonicity of Φ, this is a quasilinear parabolic equation for the unknown s. Equation (1.3) with its (possibly) degenerate coefficient functions k and Φ played an

important role in the development of analytical tools, comparable to that of minimal surfaces or mean curvature flow.

Equation (1.3) with a strictly positive coefficient function k and a strictly monotone differentiable coefficient function Φ is a non-degenerate quasilinear parabolic equation. Existence and uniqueness results for an initial-boundary value problem can be obtained in a quite straightforward way and no surprising qualitative effects can be observed. But the derivation of the equation suggests that the coefficient functions have other properties.

On the physics of (1.3).
Small diffusion. A dry medium is not permeable. This is due to the fact that there are no connected water channels inside the porous medium that can transport water. As a result, the permeability function $k : s \mapsto k(s)$ satisfies $k(0) = 0$, there is only little diffusion for small values of s. This can lead to the formation of a free boundary between areas with a positive and areas with a vanishing saturation.

Large diffusion. In a fully saturated medium ($s \equiv 1$), the value of the pressure is not determined: The water pressure in a fully saturated rock sample can be increased to any value. This fact means that the function Φ should be considered to be multivalued, it has vertical parts. We note that a large derivative of Φ implies that fast diffusion occurs in (1.3). Also the multivalued character of Φ can lead to the formation of free boundaries, namely the one of the groundwater table: In a crude approximation (namely: neglecting the capillary pressure), the pressure is arbitrary in the saturated flow below the groundwater table and it is essentially zero above the groundwater table. This leads to the free boundary problem called "dam problem".

For multi-valued Φ (or an otherwise degenerate function Φ), it is often convenient to work with $\Theta = \Phi^{-1}$ and to write the left hand side of (1.3) as $\partial_t[\Theta(p)]$, the coefficient as $k = k(\Theta(p))$, and to use the pressure p as the primary unknown.

On the mathematics of (1.3). The degeneracies of equation (1.3) lead to interesting effects, most importantly to the formation of free boundaries. Many modern analytical tools have been developed originally for the porous media equation: variational inequalities, compactness results for degenerate equations, L^1-contraction methods for parabolic problems.

One must distinguish between two different degeneracies. In the static case, the large diffusion limit leads to the free boundary problem known as the "dam problem": In the fully saturated region Ω_s below the free boundary ($s = 1$ in Ω_s), the permeability $k(s)$ is constant. As a consequence, the pressure is harmonic in Ω_s. Above the free boundary (outside Ω_s), one assumes that the pressure is constant (i.e., $\Phi(s) = p_0$ for every $s \in (0, 1)$ for the atmospheric pressure $p_0 \in \mathbb{R}$). The first existence result for the dam problem was obtained by Baiocchi [7]. He already formulated the free boundary problem with a variational inequality. His result makes use of what today is called the Baiocchi transform: Instead of the pressure p, a spatial integral $z(x_1, x_2) := \int_0^{x_2} p(x_1, t)\, dt$ is used as the unknown of the problem. The general three dimensional dam problem was treated by Alt in [2]. The problem is again written as a variational inequality, existence and uniqueness are shown in the primary variables.

The second degeneracy of the porous media equation is related to a vanishing permeability, $k(0) = 0$. If we simplify (1.3) by studying the constitutive laws $k(s) = s^\alpha$ and $\Phi(s) = s$ for $\alpha > 0$ in the case $g = 0$, we are lead to the special porous media equation $\partial_t s = \nabla \cdot (s^\alpha \nabla s)$. For this famous equation, Barenblatt found explicit solutions $s = s(x, t) \geq 0$ that exhibit a free boundary between a dry region with $s = 0$ and a partially saturated region with $s > 0$. For an introduction to

the special porous media equation we refer to [93]. The case of quite general degenerate coefficient functions k and Φ was treated first in [3, 4]. The key to these existence results for the time dependent problem are new compactness methods and the Kirchhoff transformation: With the constitutive law $s = \Theta(p)$ one uses $u := \int_0^p k(\Theta(\xi))\, d\xi$ as the new unknown of the problem. The relation $\nabla u = k(\Theta(p))\nabla p$ reduces the right hand side of (1.3) to $\Delta u - \nabla \cdot (k(s)g)$. The operator is non-degenerate elliptic in the variable u.

We remark that, in parallel, tools from convex analysis were used to formulate the problem with the pair (s, p) and to show $p \in \Phi(s)$ for a monotone multi-valued function Φ, see [99]. Variational inequalities were further developed and they became the standard tool to represent free boundary problems.

The seminal paper [3] contains existence, regularity, and uniqueness results. But the uniqueness was only shown for regular solutions; this gap was closed much later in [66] with methods that are borrowed from the theory of hyperbolic conservation laws, see also [17]. The homogenization of the degenerate system is interesting since trapping effects can occur on the micro-scale, [83, 91]. We refer to [86] for more on modelling aspects and fundamental mathematical results.

2. Hysteresis effects in porous media

2.1 *Hysteresis in the p-s-relation*

Having in mind the physical arguments of Section 1.2, let us now analyze the assumption $p = \Phi(s)$. We recall that s is a macroscopic variables that provides an information about a collection of pores.

Let us consider an experiment in which the tested porous medium is sufficiently small; for small volumes, we may assume that p and s are constant in the whole specimen. Two variables can be

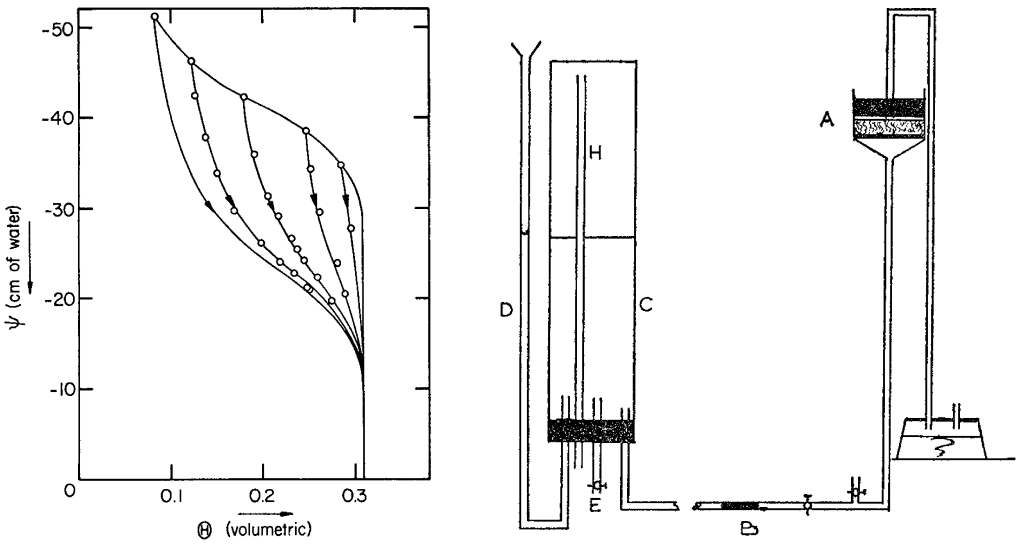

FIG. 3. Left: From Mualem [62]. Capillary pressure curves or "water retention curves". We note that in a more natural representation (flipping the vertical axis), all curves of the diagram (water pressure against water saturation) are monotonically increasing. Right: From Poulovassilis [75]. Apparatus for the measurement of the capillary head.

measured: the total saturation S (proportional to the total amount of water in the test volume, an integral over s), and the pressure P (the value of the constant function p). Poulovassilis describes such an experiment in [75], the right part of Figure 3 shows his sketch of the experimental set-up. A piece of rock (A) is in contact with water (below the rock). A tube connects the water with a reservoir (C). Since the rock absorbs water, one can lift the rock above the water level of the reservoir, the capillary forces of the pores lift the water to the higher level. The difference of the two levels is the "suction" of the porous medium. It is proportional to the pressure P (after normalizing the atmospheric pressure to 0). Lifting the rock higher, we can imagine that some water leaves the rock: The large pores do not exert any longer the necessary capillary force. We therefore have a loss of S when P is increased (in absolute value). Measuring S and P, the experiment yields a curve Φ with $P = \Phi(S)$.

A result of such an experiment is shown in the left part of Figure 3: Starting with the rock position at the water level of the reservoir ($\Psi \cong P = 0$) one has maximal saturation ($\theta \cong S \approx 0.31$). Lifting the rock to a level of 50 cm above reservoir level ($\Psi = -50$), the saturation Θ decreases to a value below 0.1.

Hysteresis is observed when the process is reversed: Saturation and pressure do not follow the same curve. Instead, lowering the rock such that imbibition takes place, the water content Θ at level, say, 30 cm, is much lower than it had been during the drainage process at 30 cm (0.13 instead of 0.3). This is the fundamental observation of hysteresis in porous media.

Understanding the effect is very important in applications such as oil recovery or CO_2-storage. The first modelling attempts have been made in the 1950s, but modelling and analysis of porous media hysteresis is an active field of research until today.

2.2 *Three effects that lead to hysteresis*

We next sketch three effects that are regarded as the main sources of hysteresis in the p-s-relation. The first concerns a physical law which enters the microscopic description of interfaces: the law for the contact angle for preceding and receding contact lines. The second regards the bottle-neck effect, which is generated by the complex geometry of the porous medium; models for this effect are the basis for most of the conceptual hysteresis laws. The third principle is again related to geometrical considerations: the full model should take into account trapped water and trapped gas.

(i) *The contact angle is velocity dependent.* It is very difficult to model dynamic contact angles. Only the static approximation is simple: The free interface between the two fluids tends to minimize the total contact energy (the sum of the energies that are attributed to the three interfaces fluid 1–fluid 2, fluid 1–solid, fluid 2–solid). When the interfaces minimize this energy, all interfaces hit the solid at a fixed angle, which is determined by the three materials.

Measurements indicate that the dynamic contact angle depends on the direction in which the interface moves. The effect is sometimes called "rain-drop effect": A rain-drop that moves down an inclined plate has a different contact angle at the front (the bottom part) than at the rear (the top part), see left of Figure 5. The detailed analysis includes many effects that cannot be discussed here: precursor films, the roughness of the solid surface (related to the lotus-effect), the disambiguation between microscopic and macroscopic contact angle.

Let us take it as an experimental fact that the contact angle depends on the velocity and, furthermore, in good approximation, only on the direction of the motion. In a porous medium this means that, even if all interfaces were spherical caps in straight tubes, we see an hysteresis effect,

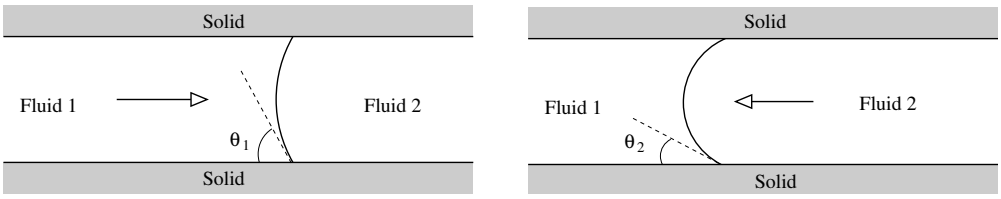

FIG. 4. The contact angle is velocity dependent. As a result, the curvature of the meniscus is different for imbibition and for drainage.

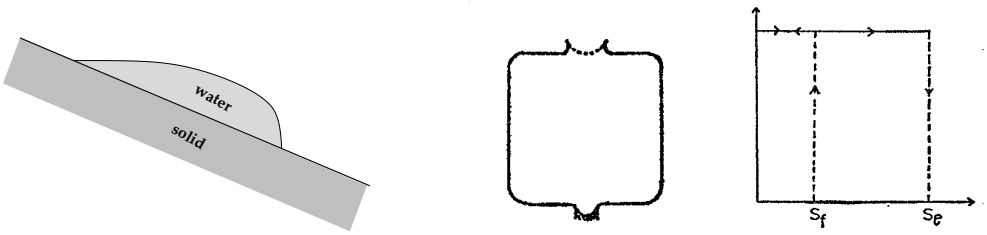

FIG. 5. Left: Sketch of a rain-drop, motivating the name "rain-drop effect" for the velocity dependent contact angle. Right: The "bottle-neck effect" in an illustration from [75] with a classical ink-bottle. The ink-bottle acts as a relay: it takes a high suction S_e to empty the ink-bottle and a lower suction S_f to fill the ink-bottle (note that the suction is $|p|$, the positive difference of water levels).

see Figure 4: If fluid 1 enters the medium (motion to the right, imbibition), a low curvature and hence a low pressure difference is observed (if fluid 1 is water, the material is hydrophillic; for air pressure 0, the water has a negative pressure, small in absolute value). If fluid 1 leaves the medium (motion to the left, drainage), a high curvature of the meniscus and hence a high pressure difference is observed (the negative pressure of the water is high in absolute value).

Let us cast this thought-experiment into formulas: We are given two material laws, Φ_{low} and Φ_{upp} (connected to the different contact angles). The water pressure can take values between the two extremes,

$$p(x,t) \in \left[\Phi_{\text{low}}\big(s(x,t)\big), \Phi_{\text{upp}}\big(s(x,t)\big)\right]. \tag{2.1}$$

The law is complemented with a condition of Kuhn-Tucker type: For an increasing saturation s, the upper value must be attained, for a decreasing saturation s, the lower value must be attained. When s is not changing with time, the pressure can have any value in the interval.

(ii) *The bottle-neck effect.* The effect was already studied around 1930, see [32, 33]: For a fixed contact angle, the water-air interface in an undulated tube has a discrete set of positions that correspond to one given pressure, compare Figure 6. The movement from one such position to the next occurs in fast processes, Haines calls them "per saltum movements" and "quantum jumps", later on they were called "Haines jumps". For an older illustration see also the right part of Figure 5, where a pore is drawn as a classical ink-bottle. Richards refers to the analysis of Haines and writes in [79]:

> [...] the height to which a liquid stands in such a tube depends on whether the liquid is first raised and allowed to sink to its equilibrium level or whether the liquid rises of

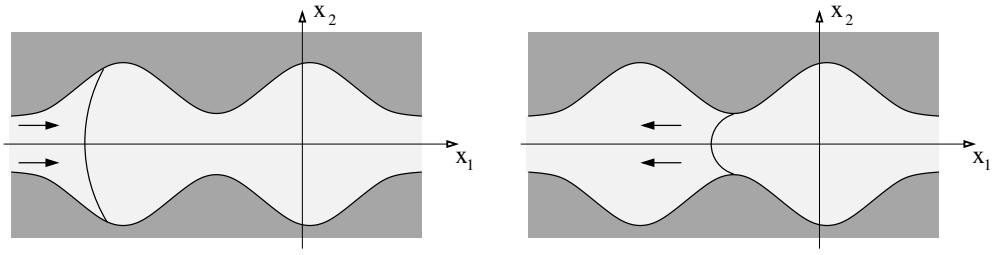

FIG. 6. A tube with narrow and wide parts. In the left figure, the interface is at a wide point of the pore, curvature and pressure are low (in absolute value). In the right figure, the interface is at a narrow point, curvature and pressure are high.

> itself to the rest position. [...] (in) a mass of soil [...] some of these tubes would have a varying cross-section and hence a hysteresis effect might be expected.

Let us describe the effect with the help of Figure 6. The hydrophillic fluid is on the left of the interface (water), the hydrophobic fluid on the right (air, with constant pressure 0). The capillary pressure induces a negative fluid pressure near the interface, hence water is sucked in by the tube. Water intake continues until a wide position is reached; at this point, the process may stop since the suction is not sufficient to pull in more water (against other forces, e.g., gravity). The imbibition pressure is therefore low in absolute value, see the left part of Figure 6. In contrast, let us study a drainage process: An external force pulls water out, the interface moves to the left until it reaches a point with a large suction; at such a narrow point, the water cannot be removed any further. As a result, the pressure for drainage is higher (in absolute value) than for imbibition.

A mathematical analysis of a dynamic process in such undulated tubes was performed in [81]. In a special geometry it is shown that only the widest and the narrowest points of the tube are of importance: For increasing saturation of the hydrophillic fluid, only the lowest pressure matters, for a decreasing saturation, only the highest pressure matters. The pressure has one value for imbibition, another for drainage. The result is once more the law (2.1).

(iii) *Snap-off effect.* This effect refers to the formation of residual fluid volumes in the porous medium. If these volumes are not any more connected with the fluid transporting channels, the residual fluid cannot be removed (unless it becomes again connected with the network).

The effect is difficult to model. While in the other two effects we observe the possibility of flat parts of the pressure function (at the same saturation, different values of the pressure can be observed), the snap-off effect can lead to flat parts of the saturation function: At the same pressure value, different saturation values can be observed. These values depend in a complex way on the history of the process. Compare Figure 7 for an illustration, once more in a tube geometry.

2.3 *Empirical approaches to model hysteresis*

We want to mention only briefly some approaches that are not concerned with a conceptual description of hysteresis. In these approaches, one tries to provide formulas to calculate hysteresis processes.

An example in this direction is [87], where all drainage and wetting curves (monotone relations in the s-p plane) are parametrized. Adapting the parametrization constants, also secondary drainage

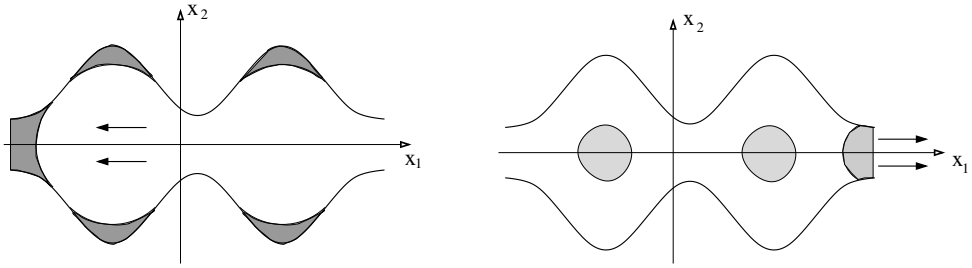

FIG. 7. Two effects in which the dark fluid remains trapped and cannot be removed from the porous medium. They lead to residual water (or oil) content and to an irreversible process. Left: When the non-wetting fluid (white) enters the pores, some of the wetting fluid (dark) remains trapped. Right: Also when a *wetting* fluid (white) pushes out a *non-wetting* fluid (dark), residuals may remain.

and wetting curves are described with the same family of curves. The numerical code determines for each point x in space the constants that describe the current process at this point. Following the corresponding path in the s-p plane, one introduced a model for hysteresis.

A similar approach is taken in [36]: Every drying or wetting process, primary, secondary or of higher order, is described by a shape function. The scaling of the shape function is characterized by five parameters. If a process is reverted, adequate five parameters are chosen and the solution follows the corresponding s-p relation.

In [47] the aim is to provide closed form expressions for the conceptually derived formulas of Mualem (that we discuss in the next section). Some quite crude interpolation algorithms are compared in [42]. In [44], the curves are fitted with third order polynomials and the behavior of the system is investigated numerically. The numerical investigation of a hysteresis model is also performed in [68].

3. Domain models for capillary hysteresis

The name "domain model" is inspired by magnetic hysteresis, where distinct domains inside a ferromagnet have a uniform magnetization. Even though switching processes are more complicated in ferromagnets (since the domain walls can move), the name "domain" was used to describe a switch that can be either in state I or in state II.

3.1 *Independent domain model*

The porous medium as a collection of switches. Many ideas are collected 1955 by Enderby in the very accessible article [25], where ideas of Everett [27, 28] are summarized and extended. We describe these ideas with the notation of the original works. Enderby starts with the observation that hysteresis in a physical system is related to the existence of meta-stable states. The presence of meta-stable states implies that, at the same macroscopic quantity λ (in our case the pressure, $\lambda \cong p$), at every point α, two states are possible (in principle), $x_\alpha^{(1)}(\lambda)$ and $x_\alpha^{(2)}(\lambda)$. In the porous media application, these are two possible local saturation values, $x \cong s$. The index α labels the "domain", a collection of atoms (here: pores) on a mesoscopic scale. Enderby demands that the domain is large enough to be independent of thermal fluctuations, but small enough such that a discontinuous behavior of the domain α still allows the macroscopic evolution to appear continuous.

Every microscopic element α has two parameters Λ_α and Λ_α^*. For increasing λ, at $\lambda = \Lambda_\alpha$ the system in the point α switches from the curve $x_\alpha^{(1)}$ to the curve $x_\alpha^{(2)}$, from state I to state II. Conversely, for decreasing λ, at $\lambda = \Lambda_\alpha^*$, it switches from $x_\alpha^{(2)}$ to the curve $x_\alpha^{(1)}$. The macroscopic quantity $X \cong s$ in its dependence on $\lambda \cong p$ is obtained by summing over the domains as

$$X = \sum_{\alpha,\ \text{domains in state I}} n_\alpha x_\alpha^{(1)}(\lambda) + \sum_{\alpha,\ \text{domains in state II}} n_\alpha x_\alpha^{(2)}(\lambda)\,, \tag{3.1}$$

where n_α is the number of domains that are identical and have the properties that are labelled by α. Finally, Enderby describes how to determine graphically from the parameter-curves Λ_α and Λ_α^* those domains α that are in state I and in state II (in dependence of the history of λ).

We recognize in Enderby's description what mathematicians call a Relay (switch from $x_\alpha^{(1)}$ to $x_\alpha^{(2)}$ and back), the averaging procedure is the one of the Preisach model (we note that also an integral version of (3.1) is provided by Enderby). Also the Preisach plane graphical analysis is (re-)invented (we recall that the work of Preisach is 20 years older than that of Enderby).

More specific to porous media modelling is Poulovassillis [75]. He uses the above model to describe the relation between the two parameters s and p (in [75] they are called water volume V and the suction S). The collection of switches is labelled with the two parameters of lower and upper switch point (the two corresponding suction values), and a function F of these two parameters indicates the proportion of this type of switch. The author speaks of an "independent domain theory", since the switches act independently. Poulovassillis describes nicely the corresponding experimental set-up (see Figure 3), explains how the density function F can be read off from experimental data and how F can be used for predictions. He provides sketches of pore geometries that explain hysteresis and also a sketch of two connected pores that do *not* behave like a switch. The latter is possible since the two pores are not independent.

An experimental test of the independent domain model was performed in 1966 by Topp and Miller [90]. Essentially, their result is that the theory performs poorly, even for artificial (glass-bead) porous media.

The similarity assumption of Philip and Mualem. The hysteresis model of Poulovassillis [75] (we recall that it is an interpretation of the Preisach model) was not easy to apply, since the density function F cannot be determined: A typical experiment yields an imbibition and a drainage curve – possibly one secondary hysteresis loop. It is not possible to reconstruct the density function F from these curves.

We change the notation slightly and use now the one of Philip [71]: The two switching values are now α and β and the distribution function is $f = f(\alpha, \beta)$. Philip introduced an assumption, namely that the distribution function for the lower switching values $f(., \beta)$ has the same shape for all β. He writes his "similarity assumption" as

$$f(\alpha, \beta) = -g(\beta)H(\alpha/\beta)/\beta\,. \tag{3.2}$$

Under this similarity assumption, the two-dimensional field f is already determined with two curves, g and H. The assumption made it possible to extract all model parameters (namely g and H) from experimental data.

The idea was made popular with the contributions of Mualem, who also had the aim to derive practical formulas. In [60] and [61], the two parameters Λ_α and Λ_α^* receive a very tangible meaning.

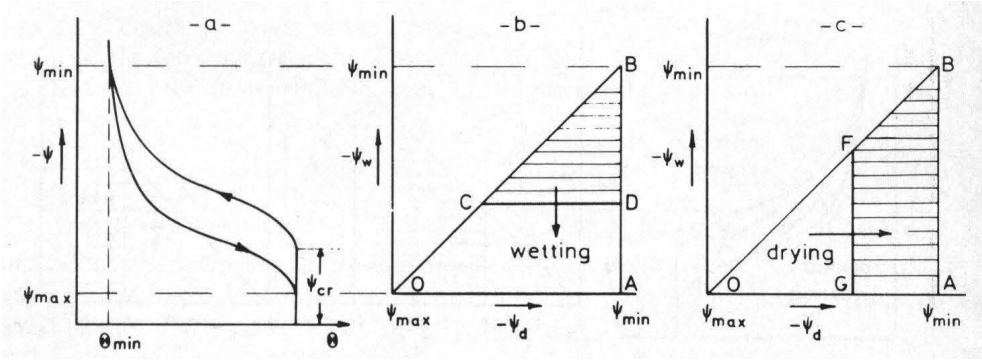

FIG. 8. Active regions for various switches from Mualem [60]. In b and c, the horizontal coordinate axis is $-\Psi_d$, the pressure value at which drainage occurs (the upper switching value). The vertical coordinate axis is the wetting pressure $-\Psi_w$ (the lower switching value). In a wetting process, a horizontal line moves downward (the height is the macroscopic pressure at every time instance), all switches above the line are flipped (the pores are filled). In a drying process, a vertical line moves right (the horizontal position is the macroscopic pressure at every time instance), all switches left of the line are flipped (the pores are emptied).

Two parameters ρ and r are introduced, they are measures for the size of the pore openings. In a wetting process, ρ indicates the pressure at which the pore is filled with water. In a drainage process, r indicates the pressure at which the pore is drained. One of the basic model assumptions is that gas and fluid phase are connected to every pore; in this way the pore is immediately filled or emptied at certain pressures. In the practical use of the model one has to determine the distribution $f = f(r, \rho)$ of pores. In order to have less parameters, Mualem uses the similarity assumption in the form $f(r, \rho) = h(r)l(\rho)$. The result is a formula for all hysteresis loops: From two boundary loops, all relevant data of the model can be obtained and a "rational interpolation formula" is created (this name for what is done by Mualem is used in [67]).

Model II of [61] differs from Model I of [60] through the fact that "trivial switches" are introduced, switches for which entry and exit pressure are identical. These pores make a reversible contribution, which is formulated in Model II by extending the distribution function $f(r, \rho)$ to arguments with $r > \rho$. Mathematically equivalent would be to introduce a finite contribution of the $f(r, r)$-values, i.e., a measure-valued part of f on the diagonal in the (r, ρ)-plane.

The aim of Parlange in [67] is to use the knowledge of only one boundary curve to obtain all relevant data (this is achieved by exploiting the knowledge of a derivative). This means that an extrapolation rather than interpolation is performed. With this method, quite irregular scanning curves can be obtained. For a more recent contribution on the reconstruction of density functions we refer to [76], where a calculation procedure is suggested that is based on three measured curves. A thorough fitting procedure of the Preisach model to experimental data can also be found in [29], where also a detailed description of the Preisach model (= independent domain model) is included.

3.2 *Dependent domains and additional variables*

The fundamental assumption of domain independence (the independence of the different switches) is related to the physical principle that, in any state, every pore has access to water (to get filled) and access to air (to get drained). This is not always the case, blocking by neighboring pores can occur.

While this is a relevant problem regarding the access to air, it is observed in [63] that the everlasting access to water seems to be a reasonable assumption (in a hydrophillic medium).

One model that includes the blocking effect has already been suggested by Everett: He introduces two weight functions P_d and P_w such that, during a drying process, not f is integrated over the region of activated switches, but the function $P_d \cdot f$ (to take into account only those switches that have access to air). The model is applied by Topp in [89] and further analyzed in [63]. A deficiency of that model (denoted as model III by Mualem) is the requirement of many measured data; this problem is resolved in [62], where an explicit formula for one of the functions reduces the number of model parameters.

The analysis of Enderby in [26] starts from physical considerations: if two switches with indices α and β are neighbors in space, then the state of switch β influences the two switching values Λ_α and Λ_α^* of switch α. The formula (3.1) can still be used to relate the macroscopic quantities λ and X, but it is more difficult to determine for which α the switch α is in state I.

Additional variables. The domain model relies on the consideration of empty and filled pores. But many more processes occur in the porous medium and it seems to be desirable to improve the model by taking more effects into consideration. One attempt is to model the snap-off effect of Section 2.2 (iii) and to introduce a "trapped saturation" as an additional state variable, see, e.g., [37]. A further effect regards the connectedness properties of filled pores. This is taken into account in a model of [20], where percolating and nonpercolating phases are modelled separately.

Another extension of the model uses the interfacial area as an additional variable. This approach is rooted in the observation that a fixed saturation s can be realized with quite different geometries: either with water in large clusters (small water-air interface), or with water scattered in a fine pore network (large water-air interface). Using interfacial area as an additional variable, one can take into account that the medium behaves differently in the two configurations. Complex re-distribution mechanisms can be modelled, see, e.g., [31, 43].

Today, some of the extended models are studied extensively. Research is concerned with modelling aspects (closure assumptions for the additional variables), parameter extraction methods, but also analytical tools (see, e.g., [74]).

3.3 *Combination with flow equations*

So far, we essentially discussed only the hysteretic relation between p and s in a given spatial point $x \in \Omega$ (averaged quantities in the macroscopic variable). In this short section we indicate some contributions concerning the combination of hysteresis with the flow equation. In particular, we want to explain why there are models that include hysteresis in the diffusion constant.

In [72], the diffusion equation (1.1) is considered for a horizontal column, i.e., for $x \in \mathbb{R}$ and $g = 0$. It is observed that, during a wetting process, some relation $p = \Phi_w(s)$ holds and, during a drying process, $p = \Phi_d(s)$ holds. Differentiating this relation, we may reduce (1.1) to $\partial_t s = \partial_x(k(s)\Phi_w'(s)\partial_x s)$ for wetting and to $\partial_t s = \partial_x(k(s)\Phi_d'(s)\partial_x s)$ for drying. In this sense, one may think of (1.1) as a standard parabolic problem and state that the diffusion constants $D_w(s) := k(s)\Phi_w'(s)$ and $D_d(s) := k(s)\Phi_d'(s)$ are different for imbibition and drainage. For this reason, other publications such as, e.g., [73] assume the diffusion parameter to be hysteretic.

Another observation of [72] is that hysteresis is important only in redistribution processes (in contrast to pure imbibition or pure drainage processes). The initial condition in [72] is a constant high saturation on the left part of the horizontal column ($x < 0$) and a constant low saturation on

the right part ($x > 0$). It is investigated how the redistribution of the water occurs; hysteresis is only present in the fact that the diffusion parameter is $D_d(s)$ in the left part and $D_w(s)$ in the right part. We will encounter higher dimensional redistribution problems in Section 5.2.

When a 3-dimensional situation is averaged in vertical direction to obtain a 2-dimensional model, one assumes that an equilibrium situation is obtained in every point of the 2-dimensional plane. Averaging accordingly the capillary pressure curves for imbibition and drainage, one obtains two effective curves. For a simple hysteresis model using a single switch in every point, the corresponding averaged curve is calculated in [21].

4. Mathematical analysis of hysteresis models

A fundamental first step in the mathematical analysis of hysteresis models is to write hysteresis operators as maps on time dependent function spaces and to investigate their properties. It seems that such a viewpoint was first taken in 1966 [13] and then fully developed by the Russian school around Krasnoselskiĭ and Pokrovskiĭ around 1970 [48].

An effect of hysteresis is that some sort of memory is present in the system. Denoting the input by u (the pressure p in the porous medium) and the output by w (the saturation s in the porous medium), the hysteresis operator is a map $u \mapsto w$, where $w(t)$ depends on the whole history of u. *Continuous* hysteresis can be described with a map

$$C\big([0,T],\mathbb{R}\big) \ni u \mapsto w \in C\big([0,T],\mathbb{R}\big)\,. \tag{4.1}$$

We tacitly assume that the operator is causal, i.e., that $w(t)$ depends only on $u|_{[0,t]}$. Not every hysteresis operator maps into the space of continuous functions, e.g., a finite superposition of Relays does not. On the other hand, under assumptions on its weight function, the Preisach operator maps in the space of continuous functions, see, e.g., [15, 49].

Here are some other properties that hysteresis operators may have: rate independence, irreversible path property, piecewise monotonicity, Hilpert's inequality. For mathematically oriented overviews we refer to [51, 57, 98, 102].

4.1 *Mathematical description of Relay and Preisach operator*

We describe here the Relay operator (more precisely: "delayed Relay", in this text often also denoted simply as "switch"). In a second step, the Preisach operator is constructed as a superposition of Relays. These constructions are outlined in many textbooks, we follow here mainly [98] and [14]. We will sketch mathematical results and the relations between different models. With this aim, we recall also the construction of the building blocks.

The Relay hysteron. We are given an input variable u and an output variable w, both are assumed to be scalar. Since hysteresis describes a memory dependent effect, we have to regard the input as a time evolution: For some time horizon $T > 0$ we assume that we are given a continuous function $u : [0,T] \to \mathbb{R}$. Our aim is to construct the output $w : [0,T] \to \mathbb{R}$. The right part of Figure 1 essentially describes how w is constructed from u. The only further information that we need is an initial condition for w, i.e., the position of the switch at time $t = 0$; we denote this value by $\xi \in \{-1,+1\}$.

Before we write down a formula for $w(t)$, let us describe in words how we want to define the output: If the input u has never taken one of the two values ρ_1 and ρ_2, then the output should still

be ξ. Otherwise, let $S_t \in [0,t]$ be the last time instance when u had the value ρ_1 or ρ_2. In the case $u(S_t) = \rho_1$, the last switching process was from $+1$ to -1 and we set $w(t) = -1$. If $u(S_t) = \rho_2$, we set $w(t) = +1$. In formulas: With $X_t := \{\tau \in [0,t] : u(\tau) = \rho_1 \text{ or } u(\tau) = \rho_2\}$ we set $S_t := \max\{\tau \in [0,t] : \tau \in X_t\}$ if $X_t \neq \emptyset$ and

$$w(t) := \begin{cases} \xi & \text{if } X_t = \emptyset\,, \\ -1 & \text{if } u(S_t) = \rho_1\,, \\ +1 & \text{if } u(S_t) = \rho_2\,. \end{cases} \tag{4.2}$$

The Relay operator is defined as the corresponding map h_{ρ_1,ρ_2} that maps an input $u \in C([0,T],\mathbb{R})$ and an initial value $\xi \in \mathbb{R}$ to an output $w : [0,T] \to \mathbb{R}$. We write $w \equiv h_{\rho_1,\rho_2}(u;\xi)$ as a function on $[0,T]$, i.e.,

$$w(t) = h_{\rho_1,\rho_2}(u;\xi)\,(t) \quad \forall t \in [0,T]\,. \tag{4.3}$$

Properties of the Relay hysteron.. The Relay operator shares some of the properties that are also observed in many systems with hysteresis (for precise statements see, e.g., [98, Chapter IV]): (1) Order preservation of h_{ρ_1,ρ_2} in u: Larger inputs create larger outputs. (2) Semigroup property: Two processes, one performed after the other, produce the same output as the combined (longer) process. (3) Piecewise monotonicity: If u is increasing on some time interval, also w is increasing on that time interval. (4) Rate independence: If we run the process $t \mapsto u(t)$ faster, the output w is the same, we only run the output faster. In formulas: Let the monotonically increasing continuous map $\varphi : [0,\tilde{t}] \to [0,t]$ be a parametrization of the time domain. We consider the output $w(t) = h_{\rho_1,\rho_2}(u;\xi)\,(t)$ on the original interval $[0,t]$ and, for the re-parametrized input $\tilde{u}(\tilde{\tau}) = u(\varphi(\tilde{\tau}))$ on $[0,\tilde{t}]$ the output $\tilde{w}(\tilde{t}) = h_{\rho_1,\rho_2}(\tilde{u};\xi)\,(\tilde{t})$. Then there holds $\tilde{w}(\tilde{t}) = w(t)$.

Some more advanced properties are related, e.g., to measurability properties or estimates of w in BV, the space of functions with bounded variation. An interesting aspect of the Relay is that, in order to determine an output $w(t)$, we do not need to know the whole process $u : [0,t] \to \mathbb{R}$, but we only need to know the sequence of local maxima and minima of u ("reduced memory sequence").

Application to capillary hysteresis. The single Relay models a single pore, the input u is the pressure p and the output w is the local water content (we note that, in the application, the output should be non-negative, the Relays should be normalized to have outputs 0 and 1). The value ρ_1 stands for the pressure value at which the pore is drained. If the input pressure $p \cong u$ takes this value, the local water content w (which contributes to the saturation) is lowered. Vice versa, at the pressure value ρ_2, the pore is filled and the local water content w is increased.

The Preisach operator. The Preisach operator is constructed by a superposition of Relays h_{ρ_1,ρ_2}. The set of all admissible pairs (ρ_1,ρ_2) is given by the restriction $\rho_2 > \rho_1$, the corresponding half plane is called the Preisach plane $\mathcal{P} := \{\rho = (\rho_1,\rho_2) \in \mathbb{R}^2 | \rho_2 > \rho_1\}$. In order to simplify, let us restrict ourself to the initial condition that all switches are initially in position $+1$ (every pore is filled). Let us furthermore assume that the weight is given by a continuous function $\mu : \mathcal{P} \to [0,\infty)$. Then the Preisach operator $\mathcal{H}_\mu$ for the weight μ is defined as

$$\mathcal{H}_\mu(u)\,(t) := \int_{\mathcal{P}} h_\rho(u;+1)\,(t)\;\mu(\rho)\,d\rho\,. \tag{4.4}$$

In order to have a simple formula, we assume here that μ is a function, but for applications it is often necessary to generalize to a measure $\mu \in \mathfrak{M}(\mathcal{P})$. This generalization allows for example to consider a finite number of Dirac measures as distribution μ, which corresponds to the superposition of a finite number of switches.

Geometric interpretation of the Preisach operator. We already described the geometric interpretation in Section 3.1, see Figure 8. For a more detailed sketch see Figure 9. To facilitate the comparison, we keep the choice of coordinate axes of Mualem from 1974: Using ρ_2 as the horizontal coordinate and ρ_1 as the vertical coordinate, the Preisach plane $\{\rho = (\rho_1, \rho_2) | \rho_2 > \rho_1\}$ is the lower right half plane. The shaded region marks those switches (ρ_1, ρ_2) that are in state $+1$, the other switches are in state -1. As the input increases (indicated by the two arrows, $\partial_t u(t) > 0$), those switches with the high switch value $\rho_2 = u(t)$ change from -1 to $+1$. Graphically, the vertical line at $u(t)$ moves to the right and all switches to the left of it have been changed to the value $+1$.

When the process is reversed and $u(t)$ is lowered ($\partial_t u(t) < 0$), those switches are flipped from $+1$ to -1 that have the low switch value $\rho_1 = u(t)$. This corresponds to a horizontal line at height $u(t)$ such that all Relays above the line are switched back to -1. Let us denote by $A(t) \subset \mathcal{P}$ the set of those Relays (ρ_1, ρ_2) that have the value $+1$ at time t. After multiple reversions of the process, the boundary of $A(t)$ forms a zig-zag line that consists of vertical and horizontal pieces. The boundary of $A(t)$ (more precisely: the part inside $\mathcal{P}$) encodes the information that the Preisach operator has about the history of the process.

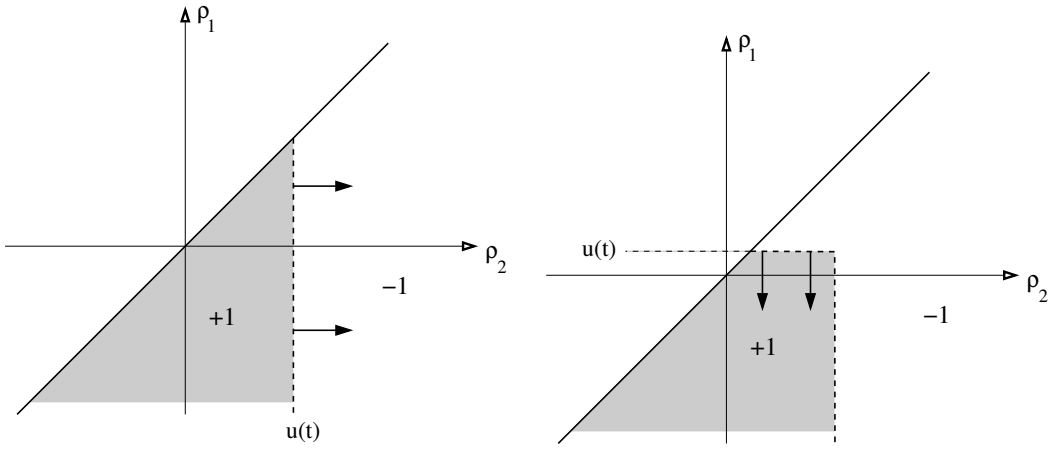

FIG. 9. The Preisach plane. Left: An increasing input function u results in flipping all switches along a vertical line at position $u(t)$. Right: A decreasing input function u results in flipping all switches along a horizontal line at vertical position $u(t)$.

Application to capillary hysteresis. The idea of combining switches to obtain a quite general hysteresis operator (to model magnetism) goes back to [104] and (with its geometric interpretation) to [77]. Everett and Enderby use the same model in the context of capillary hysteresis, calling it "domain model" (they do not make reference to Preisach's work). Enderby gives in [25] also a graphical interpretation similar to the Preisach plane, with the difference that the single piece of

$\partial A(t)$ is not a straight line, but a curve. Instead, the geometric interpretation of Mualem (who also doesn't quote Preisach) is already as the modern one which is given above, see Figure 8.

Let us make clear that formula (4.4) is essentially the same as (3.1). The input function λ in (3.1) is the pressure, $u \cong \lambda$. The single switch is labelled by $\alpha \cong \rho$, the output value of the single switch is either $x_\alpha^{(1)} \cong -1$ or $x_\alpha^{(2)} \cong +1$. Since the weight $n_\alpha \cong \mu$ can be chosen freely, it is no restriction to use only the two values ± 1 as outputs of the single switch.

Once that the Preisach model had been suggested to model the hysteretic behavior between p and s, the main task for the application was the identification problem: Given a hysteresis operator $\mathcal{H}_\mu$ (given by measurements of curves such as in Figure 3), find the measure (or the density) μ. On theoretical grounds, this problem has been investigated in [98], see page 129. Essentially, the result is that μ is determined by $\mathcal{H}_\mu$. In this context we recall our discussion of Section 3.1: Even though the measure μ is determined by the hysteresis operator, only the similarity assumption made it possible to reconstruct μ from experimental data.

Properties of the Preisach operator. For any finite Borel measure μ, the Preisach operator is causal and rate independent; it is therefore a hysteresis operator in the mathematical sense of [98]. For a large class of weights μ, the Preisach operator maps into the space of continuous functions. Furthermore, qualitative properties regarding minor hysteresis loops can be proved: The "congruency property" and the "wiping-out property".

Since the single Relay operator has discontinuous outputs $t \mapsto w(t)$ (even for smooth input functions $t \mapsto u(t)$), in general we cannot expect the Preisach operator $\mathcal{H}_\mu$ to provide smooth outputs w. But it can be shown that $\mathcal{H}_\mu$ maps every input $u \in C^0([0,T],\mathbb{R})$ to $w \in C^0([0,T],\mathbb{R})$ if the μ-measure of all vertical and all horizontal lines vanishes (this condition is also necessary). In particular, for measures $\mu(x)\,dx$ as described above (regular with respect to the Lebesgue measure), the Preisach operator maps into the space of continuous functions. These and more refined results are contained in [98]: uniform continuity, estimates in Hölder and Sobolev spaces, vectorial extensions and much more. A numerical approximation scheme for the Preisach model is studied in [94].

4.2 *Play hysteron and further hysteresis models*

In recent years, much research was devoted to another hysteresis model: The Play-type hysteron and the corresponding averaged system, the Prandtl–Ishlinskiĭ model.

The Play hysteron. Loops of the Play hysteron are sketched in the left part of Figure 10. Let us give a loose description of how the input u generates the output w: Within certain w-dependent bounds, u can vary freely without inducing any change of w. Once the limits are reached, w must increase with u, keeping a certain prescribed distance (or w must decrease with u, keeping the distance).

As in the Relay hysteron, there are horizontal parts in the output curve, but in contrast to the Relay hysteron, there are no jumps of the output function. The Play hysteron can be written with an ordinary differential equation (or, more precisely, with a differential inclusion). We use the multi-valued sign function $\operatorname{sign} : \mathbb{R} \to \mathbb{R}$, $\operatorname{sign}(\xi) = \pm 1$ for $\pm\xi > 0$ and $\operatorname{sign}(0) = [-1,+1]$. Denoting by $2\gamma > 0$ the width of the flat parts, we can write

$$u - w \in \gamma \operatorname{sign}(\partial_t w)\,. \tag{4.5}$$

This relation expresses with one formula that either $\partial_t w$ vanishes, in which case u is free within the interval $[w-\gamma, w+\gamma]$, or $\partial_t w$ has a sign, in which case $u = w \pm \gamma$, the sign is that of $\partial_t w$.

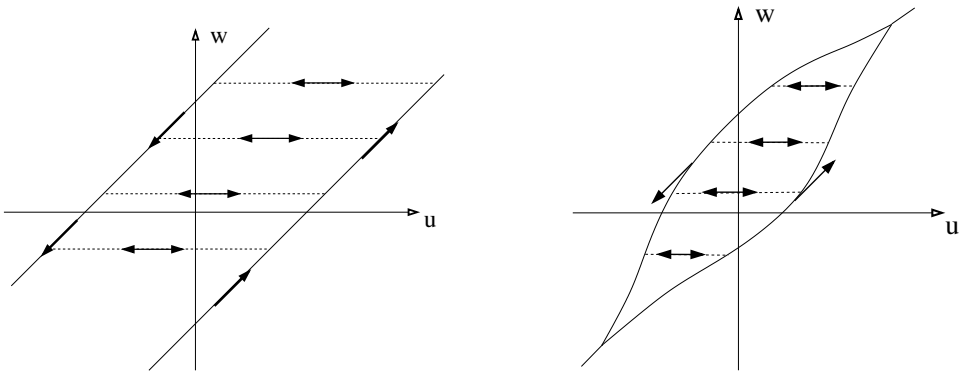

FIG. 10. Left: The Play-hysteron. In porous media, u is the pressure and w is the saturation (hence the coordinates are exchanged in comparison to Figure 3). Right: The generalized Play.

To generalize the model, the parameter γ can be chosen to depend on w. Likewise, the parameter w on the left hand side may be replaced by a function of w. With these alterations, the system (4.5) describes a *generalized Play.* The generalized Play can describe quite general loops such as the one sketched in the right part of Figure 10.

Writing the hysteron as an ordinary differential equation makes clear that no internal parameters are used: If a system starts in state (u_0, w_0) at time t_0, the evolution of $u = u(t)$ for $t \geqslant t_0$ determines $w(t)$ for $t \geqslant t_0$. The evolution is independent of any possible other parameter and it is independent of the history of u before time t_0 (semigroup property).

It can be shown that the generalized Play is a special case of a Preisach operator and hence shares all the basic properties: (1) Order preservation, (2) Semigroup property, (3) Piecewise monotonicity, (4) Rate independence. We refer to [49] or [98], where also some more specific properties are derived: Continuity properties of the generalized Play, a formulation with variational inequalities, Hilpert's inequality, and an extension to the vectorial case.

Relation to capillary hysteresis. Let us imagine the pore space as a collection of many undulated tubes as in Figure 6. Within a certain range, the pressure $u \cong p$ can vary without affecting the saturation $w \cong s$: The interface in the single tube can move the short way from the narrow to the wide part, which changes the pressure (since the curvature of the interface changes), but it does not change the (macroscopic) saturation. Once that the maximal or minimal pressure is obtained, all tubes with this maximal/minimal diameter are filled completely and the (macroscopic) saturation is affected.

Of course, the affine relation $u = w \pm 1$ between pressure $u \cong p$ and saturation $w \cong s$ for an ongoing imbibition or an ongoing drainage process must be replaced by a more realistic relation such as $p = p_c(s) \pm \gamma(s)$, which results in the generalized Play model

$$p \in p_c(s) + \gamma(s)\,\mathrm{sign}(\partial_t s)\,. \tag{4.6}$$

The main feature of the Play-type model (4.6) are the horizontal scanning curves (vertical with the choice of axes as in Figure 3). Physical arguments for this relation on the basis of the "contact angle hysteresis" are presented in [35]. Essentially, at the same saturation, the pressure can vary between two extreme values due to the varying contact angle, see Figure 4. The model was investigated in an

extended version with an additional parameter $\tau > 0$ in [9] and [10]. Formally, upon setting $\tau = 0$, these models reduce to (4.6).

We emphasize that the model can be read in two different ways. An elementary possibility is to interpret it globally: At a fixed saturation s, the pressure p can take any value between a value $p_{dr}(s)$ (the pressure on the drainage curve) and a value $p_{im}(s)$ (the pressure on the imbibition curve). If we read (4.6) in this way, we construct a crude solution to the problem of constructing secondary scanning curves: We use only vertical scanning curves between imbibition and drainage curve. We recall that the construction of scanning curves is one of the main difficulties in applications.

The more sophisticated point of view is to interpret (4.6) as a model at the scale of the pores (we recall that we also interpreted Relays as a description of pores in the domain model). We should therefore average the elementary hysteresis model (4.6) over many Play-type parameters. Just as we obtained the Preisach model from Relay hysterons, this construction provides the Prandtl–Ishlinskiĭ model from Play hysterons.

The Prandtl–Ishlinskiĭ model. We keep the notation of (4.6) and assume that for every $\rho \in \mathcal{P}$ (an abstract parameter in some parameter region $\mathcal{P}$) we are given a base function $s \mapsto p_c^\rho(s)$ and an interval function $s \mapsto \gamma^\rho(s)$. Let us assume that every pair (p_c^ρ, γ^ρ) defines a hysteresis operator $w(.) = e_\rho(u(.))$ according to (4.6) with p_c and γ depending on ρ (we suppress the initial condition). Then, for a measure μ on the parameter space $\mathcal{P}$, the Prandtl–Ishlinskiĭ operator is

$$\mathcal{E}_\mu : u \mapsto w\,, \quad w(t) = \int_{\mathcal{P}} e_\rho(u)(t)\, d\mu(\rho)\,. \tag{4.7}$$

Many properties have been analyzed for this operator, e.g., the existence of reduced memory sequences and the inversion problem. Some relations to the Preisach model can be established: if the density function μ of the Preisach model is supported on a graph, then the Preisach model is equivalent to a Prandtl–Ishlinskiĭ model. Vice versa, under technical assumptions on the parameters, every Prandtl–Ishlinskiĭ model can be written as a Preisach model, see Chapter IV in [98].

Other models. The *Stop-hysteron* is a variant of the Play-hysteron. In the Stop-hysteron, free movements are allowed as long as the difference $u - w$ remains constant, and w cannot exceed a certain value. Upon a normalization, we may write

$$w \in \operatorname{sign}\big(\partial_t(u - w)\big)\,. \tag{4.8}$$

The Stop-hysteron is closely related to the Play-hysteron: Introducing $\tilde{w} := u - w$ in (4.5) with $\gamma = 1$, we find the relation $\tilde{w} \in \operatorname{sign}(\partial_t(u - \tilde{w}))$, hence the pair $(u, \tilde{w})$ satisfies (4.8). A superposition of Stops is called a *Prandtl–Ishlinskiĭ model of Stop-type.*

Of a quite different nature is the Duhem model of hysteresis, which has some undesired properties and is therefore not used in the modelling of porous media. For more on the model we refer to [98, 103].

4.3 *Partial differential equations coupled to hysteresis operators*

Among the earliest investigations of partial differential equations coupled to hysteresis are [95, 96]. The contribution [95] deals with the parabolic problem $\partial_t w + Au = f$, where A is an elliptic operator such as $-\Delta$ and a relation $w = \mathcal{E}(u)$ expresses the hysteretic dependence of w on u.

Under restrictive assumptions on the hysteresis operator $\mathfrak{E}$, an existence result is derived, the proof is performed by time discretization. Essential for the limit process are a priori estimates for time discrete solutions. These estimates rely on a careful exploitation of monotonicity properties of the hysteresis operator.

A similar model is provided by the equation

$$\partial_t(u+w) - \Delta u = f\,, \tag{4.9}$$

accompanied by the hysteretic dependence $w = \mathfrak{E}(u)$. Equation (4.9) must be solved on the space-time cylinder $\Omega_T = \Omega \times (0,T)$. The hysteresis relation must be interpreted as $w(x,t) = \mathfrak{E}(u(x,.))(t)$ for almost every $x \in \Omega$ and almost every $t \in (0,T)$. In this setting, quite general hysteresis operators can be studied, e.g., the Preisach operator. For existence results see [97] and [98], Chapter XI, Theorem 4.1.

Let us make the connection of (4.9) to capillary hysteresis: As before, u stands for the pressure (or, possibly, its Kirchhoff transformation as in Section 1.3), $-\nabla u$ is the driving force and, for a normalized permeability, also the flux according to Darcy's law. The conserved quantity $u + w$ then stands for the saturation. The model therefore assumes a strictly monotone hysteretic relation between $p = u$ and $s = u + w$. The fact that the hysteretic relation $u \mapsto u + w$ has no flat parts helps in the analysis of the system. Furthermore, the analysis uses that coefficients are constant and, in particular, not depending on the solution (linearity of relation (4.9) in u and w).

The books [14, 51, 98] contain many more existence results for models with hysteresis. In particular, the early contributions are embedded into a larger theory and the essential ingredients for existence results are identified. One aspect regards the monotonicity of hysteresis operators: While standard L^2-monotonicity cannot be expected for hysteresis operators, the notion of *piecewise monotonicity* turns out to be useful: This property is satisfied by many hysteresis operators and it is sufficient to derive estimates for solutions. In order to obtain the uniqueness of solutions, Hilpert's inequality is used. The inequality may be stated as

$$\partial_t|w_1 - w_2| \leqslant \operatorname{sign}(u_1 - u_2)\partial_t(w_1 - w_2)\,.$$

In the original work [39], the inequality was stated for inputs u_1, u_2 and the corresponding generalized Play outputs w_1, w_2.

Results typically concern existence, uniqueness and L^1-contraction properties. Other results are on long time behavior (e.g., [45, 54] and, for an interesting ODE-problem with resonance, [52]) and control problems (compare [40] and references therein).

Beyond plasticity and porous media, a wide range of applications with hysteresis has already been treated: Phase field models [14, 40, 54], Maxwell systems [101], variational inequalities and contact problems [53], fatigue [23], transport [69]. Much work is available for hyperbolic equations, such as the (one-dimensional) dynamic plasticity equation $\partial_t^2 u - \partial_x \mathfrak{E}(\partial_x u) = f$ in [50], see also [100] and the references therein. We do not comment further on the more complex question of vector-valued hysteresis and refer instead to [98, 101].

Nonlinear porous medium equation. The nonlinear porous media equation (1.1) with a Preisach operator relation between pressure and saturation has been investigated in [5]. The authors treat the full problem with general boundary conditions, a general Preisach operator, and a degenerate coefficient $k = k(s)$. Degeneracy of k is meant in the sense of a vanishing permeability for small saturations, $k(0) = 0$, which corresponds to a lack of ellipticity in the equation. We note that

the latter makes some regularization of the model necessary, the hysteresis relation is modified by adding a monotone function β (comparable to the above "regularization" by setting $s = u + w$ instead of $s = w$).

A similar analysis is performed in [6] for a generalized Play operator in the hysteresis relation. Here, another regularization is chosen: A time convolution in the permeability coefficient k allows the derivation of an existence result.

We mention already here two existence results for the nonlinear problem in the case that the hysteresis relation is regularized with a rate-dependent term ($\tau > 0$): The nonlinear Richards equation with Play type hysteresis was studied in [55], a degenerate nonlinear system was studied in [85]. We note that the former contribution does not allow for a degenerate permeability ($k(0) = 0$), the latter contribution allows this degeneracy, but the constructions are possible due to a degenerate behavior of $p_c = p_c(s)$, which prevents the system from developing a vanishing saturation. We are not aware of any other existence result for the degenerate nonlinear partial differential equation with hysteresis.

Homogenization. A homogenization of the Preisach model is performed in Chapter XI of [98]: A Relay in every spatial point, with highly oscillatory switch parameters, results in a Prandtl–Ishlinskiĭ model in every macroscopic point. Furthermore, the coupling of the partial differential equation (4.9) to a highly oscillatory Relay relation between u and w is analyzed. The effective equation is again $\partial_t(u + w) = \Delta u$, now u and w are coupled through a Prandtl–Ishlinskiĭ model.

The problem $\partial_t s = \Delta p$ coupled to (4.6) with an affine law p_c and with $\gamma = \gamma(x)$ is treated in [82]. In the framework of stochastic homogenization, it is assumed that the (randomly chosen, ergodic) parameters of the Play-type law are different in different spatial points. For a parameter $\varepsilon > 0$ that stands for typical distances, it is assumed that the mixing of different materials is getting finer as $\varepsilon \to 0$. The result is an effective equation which is again a linear porous media equation, but now s and p are coupled with a Prandtl–Ishlinskiĭ law.

Energetic solutions. We mention that a quite different perspective on rate-independent systems was introduced with the concept of energetic solutions, see [58, 59] and the references therein. The approach has some similarities with gradient flow structures: The evolutionary system is described with two functionals, dissipation and energy. These two functionals on a Banach space encode all the information that is needed for the evolution, typically a partial differential equation with rate-independent material laws (i.e., hysteresis). The approach is extremely successful with many applications in the context of plasticity. It seems to be an interesting challenge to explore the possibilities of this new approach in the porous media area and to investigate the connections to existing results.

5. Extensions and applications, gravity fingering

5.1 *Rate-dependent effects*

Since experiments in porous media are typically performed at low rates, it is often reasonable to assume that the porous medium is in an equilibrium state in every instant of time (quasi-static evolution). This equilibrium assumption is reflected by the fact that hysteresis is a rate-independent phenomenon.

Nevertheless, some experiments demonstrate non-equilibrium effects. The most striking evidence for a rate-dependent relation between p and s is probably the effect of saturation

overshoots in imbibition problems. We briefly describe this effect below. It is not directly linked to hysteresis, but we will observe a connection with hysteresis in Section 5.2.

It seems that [9] was the first contribution in which the (rate-independent) hysteresis was combined with a dynamic term in the p-s-relation. Model (11) of [9] can be written in the form

$$p \in p_c(s) + \gamma(s)\,\mathrm{sign}(\partial_t s) + \tau \partial_t s\,. \tag{5.1}$$

The real number $\tau \geqslant 0$ is a model parameter that quantifies the rate-dependent effects. We read (5.1) as an ordinary differential equation for s: as time increases, s moves towards one of its equilibrium positions. With this interpretation, we can regard τ as a measure of typical redistribution times. Note that the rate-independent Play model (4.6) is recovered by setting $\tau = 0$.

In [9], the authors suggest the model and show that the relation provides a thermodynamically admissible model (see also [34]). In [10] the model is formulated as above, a one-dimensional existence result was proved and a numerical scheme was developed. In [55, 78] higher dimensional existence results are obtained for flow equations coupled to (5.1) with $\tau > 0$. A variety of related dynamic capillary pressure models is discussed in [65].

Saturation overshoot behind wetting fronts. Many imbibition processes involve an advancing wetting front. In such processes, the porous medium has initially a low saturation, and it has a high saturation behind the wetting front. The process can occur with a monotonic saturation profile such that, for a fixed point x in space, the saturation increases at all times. But some experiments show non-monotonic saturation profiles. In such a case (for a fixed time t the saturation profile has a local maximum near the front), we speak of a *saturation overshoot.*

The non-monotonic saturation profile cannot be explained with the standard Richards equation. We emphasize that it also cannot be explained by (only) adding hysteresis in the Richards equation: Since we consider a pure imbibition process, only the imbibition curve of the hysteresis loop is of importance in this process. Instead, equation (5.1) can produce overshoots, even without hysteresis (i.e., for $\gamma = 0$), at least in the two-phase flow context [38, 92]. A recent overview on saturation overshoot effects and their modelling can be found in [105]. The overshoot is usually interpreted as a result of redistribution effects. It can also be modelled with the additional variable of interfacial area (compare Section 3.2).

5.2 *Gravity fingering*

Gravity fingering is a beautiful experimental observation (see Figure 11) and, at the same time, an effect that depends crucially on hysteresis. In this sense, gravity fingering is an ideal test-case for hysteresis models in porous media. We sketch here the effect and its analysis.

The underlying experiment is easily described: An initially dry porous medium is wetted from the top. Under the influence of gravity, the liquid moves downwards in the porous medium. It has two possibilities to do so: (A) As a planar wetting front. In this case, the saturation of the medium increases in every point (x_1, x_2, x_3) in space and remains essentially independent of the horizontal coordinates (x_1, x_2). (B) In the form of fingers as in Figure 11. For experimental results we refer to [8, 64, 88].

Both possibilities (A) and (B) can be observed in experiments. Which pattern is formed depends on many parameters: on the medium (typical pore size, pore size distribution, material parameters and the corresponding contact angle), the initial saturation, and on the rate of the wetting process.

Without careful choices of parameters, one will typically obtain pattern (A), the fingering pattern (B) can be observed, e.g., in very dry sand at low flow rates.

Important for us is the fact that the standard model for porous media (no hysteresis) cannot explain fingering: The Richards equation has stability properties (L^1-contraction principle) that exclude fingering [17, 66]. To avoid misunderstandings: In principle, also the two-phase flow equation can explain a fingering phenomenon (in contrast to the Richards equation). But we note that the inertia of air in dry sand is extremely low. This is a clear indication that the fingering effect is not a two-phase flow effect, but has some other origin.

Hysteresis as an important factor. A simple argument makes clear that hysteresis is important for fingering, compare [24, 30]. Let us describe here the basic mechanism. The Richards equation (1.3) is always dissipative: Saturation differences lead to pressure differences and these lead to flow from high to low saturation areas. What does this imply in a situation with fingers as in Figure 11? The saturation is high in the finger and low in the space between two fingers. Dissipation leads to a flow from the finger to the dry neighborhood. Hence, without hysteresis, the fingers become wider with time. But the experiments do not show any spreading. The fingers are not wider in the top part (where they had a long time to spread) than in the bottom part.

Hysteresis is a mechanism that can prevent the fingers from spreading. Hysteresis in the s-p-relation allows for different values of s at the same pressure p. This is what we observe in the fingering phenomenon: The saturation is very different in the finger and in the vicinity, but the pressure is essentially identical (since no spreading occurs). Already the simple Play hysteresis law (4.6) makes the effect possible: For $\partial_t s = 0$, different values of s can be attained at the same value of p.

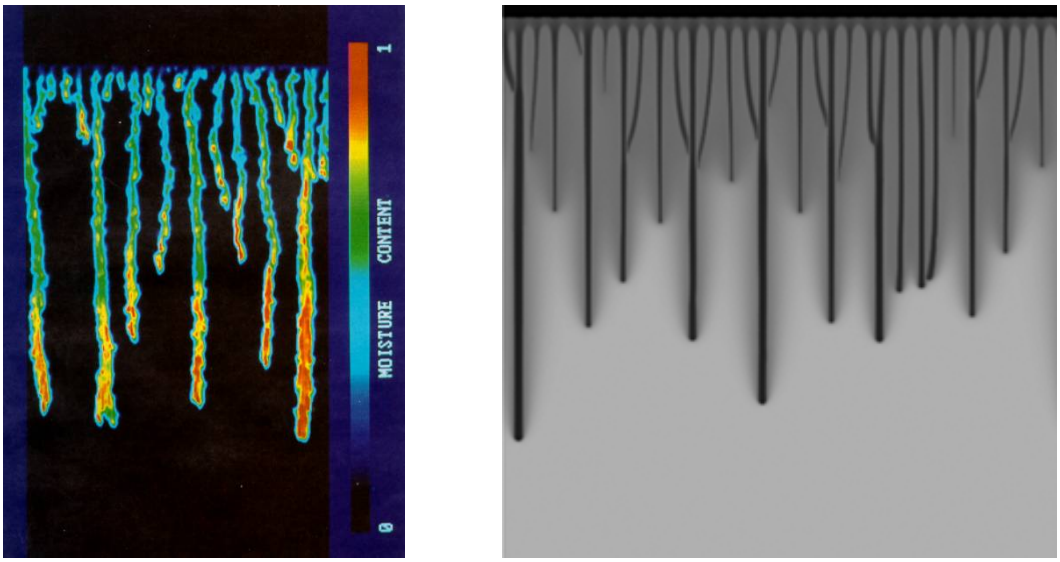

FIG. 11. Left: An experimental result for fingering in a porous medium (courtesy of R. J. Glass of the Soil and Water Laboratory at Cornell). Right: Numerical solution of a model with hysteresis and dynamic effect [78].

The possible influence of hysteresis is analyzed in mathematical terms in [84]: The Richards equation with Play-type hysteresis does not define an L^1-contraction, hence fingering is possible.

Hysteresis alone cannot explain fingering. A priori, it is not clear whether the porous medium equation with hysteresis and without dynamic term ($\tau = 0$) can explain fingering. Since we see an imbibition process in every point for all times, one might expect the strict inequality $\partial_t s > 0$ in the whole domain. In this case, hysteresis does not play a role and cannot explain the effect. The numerical evidence of [55, 78] indeed indicates that hysteresis with $\tau = 0$ does produce a more unstable behavior of the system, but it does not produce the fingering effect.

The situation changes dramatically when the dynamic term is included: $\tau > 0$ can generate a saturation overshoot in the finger-tips, which means that a drainage process takes place in the fingers behind the saturation maximum. Hysteresis sets in and explains the stability of the fingers. This argument is analyzed in [78] with one-dimensional calculations. In the same contribution, also the numerical result of Figure 11 (right) is obtained for a Play-type hysteresis model with $\tau > 0$.

Well-posedness for the Richards equation with Play-type hysteresis and dynamic term is shown in [55]; for the two-phase flow model, existence is shown in [46] and uniqueness in [16]. For a result with degenerate p_c-curve see [85]. Numerical experiments in [46, 55, 78] confirm that these models can generate the fingering effect.

Other approaches to fingering. Similar models are studied in [80]. A one-dimensional analysis of the model with $\tau > 0$ is performed to confirm the saturation overshoot. With a hysteresis model that is constructed with the help of explicit formulas for primary and secondary curves, numerical results are performed in one and two space dimensions. In one space dimension, $\tau > 0$ produces the saturation overshoot, the inclusion of hysteresis removes secondary oscillations. In two space dimensions, the profile of one finger is calculated.

Other non-equilibrium Richards equations that include rate-dependent terms have been studied, e.g., in [22, 65]. One application is that a low-frequency instability criterion can be introduced and used to predict the occurrence of an instability.

A completely different approach with a phase-field model is introduced in [19]. An "apparent surface tension" leads to the appearance of fingers. It is an ongoing discussion, whether or not the physical principles of the model are sound. In any case, the model does not fit into the framework that is discussed here.

5.3 *Further directions and open questions*

Much research has been performed on hysteresis in porous media. The main focus of the last 60 years was to develop Preisach and Play-type models for hysteresis and to couple them to the Richards equation for unsaturated porous media flow. We discussed the importance of additional dynamic terms (or other non-equilibrium extensions). In this final section, we collect some further directions of research and open questions.

Fingering. Regarding the fingering effect, many questions are open: What determines the typical diameter of fingers, what determines typical distances? Fingers essentially occur only in dry sand; is there a saturation threshold such that, beyond this threshold, no fingering is possible? A similar question can be asked with respect to the imbibition rate, which also must lie in a certain (material-dependent) range. These questions are completely open. Certainly, instability criteria as in [22, 65]

can be useful in such an analysis. We also see a connection with [52] which investigates whether or not the dissipation due to hysteresis can prevent a solution from blow up due to resonance.

Beyond Richards equations. We essentially restricted this survey to the Richards equation and its coupling to hysteresis. For two-phase flow equations we already mentioned [46], where hysteresis is introduced completely analogous to the unsaturated flow case. Another approach is taken in [56], where hysteresis is introduced with a two-state model and a hyperbolic framework is used. Coupling of porous media hysteresis with other materials is interesting, see, e.g., [41] for a coupling with an elasto-plastic material. But even the further development of the unsaturated flow equation is an interesting field when non-equilibrium effects are taken into account (e.g., the interfacial area).

Upscaling. Rigorous mathematical upscaling of a porous medium equation with hysteresis in the sense of homogenization seems to be available only under very restrictive assumptions. One either has to assume that the hysteresis law is strictly monotone [98] or that the permeability function is constant [82]. A non-rigorous result is obtained in [18]. Rigorous upscaling of general hysteresis laws in nonlinear partial differential equations is essentially open.

Energetic solutions. We already mentioned that the connection to energetic solutions should certainly be explored, since this regards the intersection of two very active fields, see Section 4.3.

Numerical methods. We did not discuss the development of numerical methods to solve the hysteresis equations. Numerical methods are used, e.g., in [46, 55, 64, 78, 80]. Our impression is that the numerical methods still must be optimized. They show slow convergence and, as of today, they do not permit three-dimensional calculations. For a recent contribution and further references, we mention [70].

Pore network models. Today, more than 80 years after the thoughts of Haines about spherical packings, resulting pore-scale geometries, and corresponding capillary pressures, the design and the analysis of pore-scale geometries has become an active field of research. With todays computer power, the geometry of a pore network can be implemented and modern algorithms allow to calculate physical quantities.

A computer experiment can be performed by specifying a geometry, contact angles, densities, viscosities, and boundary conditions. By computer experiments, one can determine permeability and capillary pressure curves and, in particular, study the hysteretic behavior. The residual saturation and the interfacial area can be calculated and one can study the dependence of these parameters on the data. We emphasize that some of these quantities are hard to measure in physical experiments. For a comprehensive overview over the state of the art in 2001 we refer to [12], for a more recent contribution and further references see [43].

References

1. Albers, B., Modeling the hysteretic behavior of the capillary pressure in partially saturated porous media: A review. *Acta Mech.* **225** (2014), 2163–2189. Zbl1302.74129 MR3237893
2. Alt, H.-W., A free boundary problem associated with the flow of ground water. *Arch. Rational Mech. Anal.* **64** (1977), 111–126. Zbl0371.76079 MR0428901
3. Alt, H.-W. & Luckhaus, S., Quasilinear elliptic-parabolic differential equations. *Math. Z.* **183** (1983), 311–341. Zbl0497.35049 MR0706391

4. Alt, H.-W., Luckhaus, S. & Visintin, A., On nonstationary flow through porous media. *Ann. Mat. Pura Appl. (4)* **136** (1984), 303–316. Zbl0552.76075 MR0765926
5. Bagagiolo, F. & Visintin, A., Hysteresis in filtration through porous media. *Z. Anal. Anwendungen* **19** (2000), 977–997. Zbl0977.35072 MR1812655
6. Bagagiolo, F. & Visintin, A., Porous media filtration with hysteresis. *Adv. Math. Sci. Appl.* **14** (2004), 379–403. Zbl1073.76066 MR2111820
7. Baiocchi, C., Su un problema di frontiera libera connesso a questioni di idraulica. *Ann. Mat. Pura Appl. (4)* **92** (1972), 107–127. Zbl0258.76069 MR0408443
8. Bauters, T. W. J., DiCarlo, D. A., Steenhuis, T. S. & Parlange, J.-Y., Soil water content dependent wetting front characteristic in sands. *Elsevier Journal of Hydrology* **231–232** (2000), 244–254.
9. Beliaev, A. & Hassanizadeh, S., A theoretical model of hysteresis and dynamic effects in the capillary relation for two-phase flow in porous media. *Transp. Porous Media* **43** 3 (2001), 487–510. MR1948682
10. Beliaev, A. & Schotting, R., Analysis of a new model for unsaturated flow in porous media including hysteresis and dynamic effects. *Comput. Geosci.* **5** (2001), 345–368 (2002). Zbl1026.76050 MR1892965
11. Bertotti, G. & Mayergoyz, I., Eds., *The science of hysteresis. Vol. III*. Elsevier/Academic Press, Amsterdam, 2006. Hysteresis in materials. Zbl1117.34047
12. Blunt, M., Flow in porous media—pore-network models and multiphase flow. *Current opinion in colloid & interface science* **6** (2001), 197–207.
13. Bouc, R., Solution périodique de l'équation de la "ferrorésonance" avec hystérésis. *C. R. Acad. Sci. Paris Sér. A-B* **263** (1966), A497–A499. Zbl0152.42103 MR0201106
14. Brokate, M. & Sprekels, J., *Hysteresis and phase transitions*, vol. 121 of *Applied Mathematical Sciences*. Springer-Verlag, New York, 1996. Zbl0951.74002 MR1411908
15. Brokate, M. & Visintin, A., Properties of the Preisach model for hysteresis. *J. Reine Angew. Math.* **402** (1989), 1–40. Zbl0682.47034 MR1022792
16. Cao, X. & Pop, I., Two-phase porous media flows with dynamic capillary effects and hysteresis: uniqueness of weak solutions. *Comput. Math. Appl.* **69** (2015), 688–695. MR3320281
17. Carrillo, J. & Wittbold, P., Uniqueness of renormalized solutions of degenerate elliptic-parabolic problems. *J. Differential Equations* **156** (1999), 93–121. Zbl0932.35129 MR1701806
18. Celia, M. & Guswa, A., Hysteresis and upscaling in two-phase flow through porous media. In *Fluid flow and transport in porous media: mathematical and numerical treatment (South Hadley, MA, 2001)*, vol. 295 of *Contemp. Math.* Amer. Math. Soc., Providence, RI, 2002, pp. 93–104. Zbl1026.86001 MR1911540
19. Cueto-Felgueoroso, L. & Juanes, R., Nonlocal interface dynamics and pattern formation in gravity-driven unsaturated flow through porous media. *Physical Review Letters* **101** (2008), 244504–1–244504–4.
20. Doster, F., Hönig, O. & Hilfer, R., Horizontal flow and capillarity-driven redistribution in porous media. *Phys. Rev. E* **86** (2012).
21. Doster, F., Nordbotten, J. & Celia, M., Hysteretic upscaled constitutive relationships for vertically integrated porous media flow. *Comput. Vis. Sci.* **15** (2012), 147–161. MR3148139
22. Egorov, A., Dautov, R., Nieber, J. & Sheshukov, A., Stability analysis of gravity-driven infiltrating flow. *Water Resources Research* **39** (2003), 12–1–12–14.
23. Eleuteri, M., Kopfová, J. & Krejčí, P., Non-isothermal cyclic fatigue in an oscillating elastoplastic beam. *Commun. Pure Appl. Anal.* **12** (2013), 2973–2996. Zbl1264.74244 MR3060919
24. Eliassi, M. & Glass, R., On the continuum-scale modeling of gravity-driven fingers in unsaturated porous media: The inadequacy of the Richards equation with standard monotonic constitutive relations and hysteretic equation of state. *Water Resources Research* **37** (2001), 2019–2035.
25. Enderby, J., The domain model of hysteresis, Part 1. *Independent domains. Trans. Faraday Soc.* **51** (1955).

26. Enderby, J., The domain model of hysteresis, Part 2. *Independent domains. Trans. Faraday Soc.* **52** (1956).
27. Everett, D. & Smith, F., A general approach to hysteresis. Part 2: Development of the domain theory. *Transactions of the Faraday Society* **50** (1954), 187–197.
28. Everett, D. & Whitton, W., A general approach to hysteresis. *Trans. Faraday Soc.* **48** (1952), 749–757.
29. Flynn, D., McNamara, H., O'Kane, J. & Pokrovskii, A., Application of the Preisach model to soil-moisture hysteresis. *Bertotti, M. (ed.) The Science of Hysteresis* **3** (2005). Zbl1136.76048
30. Glass, R., Steenhuis, T. & Parlange, J., Mechanism for finger persistence in homogeneous, unsaturated, porous media: Theory and verification. *Soil Science* **148** (1989), 60–70.
31. Gray, W. & Hassanizadeh, S., Unsaturated flow theory including interfacial phenomena. *Water Resources Research* **27** (1991), 1855–1863.
32. Haines, W., Studies in the physical properties of soil. iv. a further contribution to the theory of capillary phenomena in soil. *The Journal of Agricultural Science* **17** (1927), 264–290.
33. Haines, W., Studies in the physical properties of soil. v. the hysteresis effect in capillary properties, and the modes of moisture distribution associated therewith. *The Journal of Agricultural Science* **20** (1930), 97–116.
34. Hanyga, A. & Seredyńska, M., A dynamic model of capillary hysteresis in immiscible fluid displacement. *Transp. Porous Media* **59** (2005), 249–265. MR2132230
35. Hassanizadeh, S. & Gray, W., Thermodynamic basis of capillary pressure in porous media. *Water Resour. Res.* **29** (1993), 3389–3405.
36. Haverkamp, R., Reggiani, P., Ross, P. & Parlange, J.-Y., Soil water hysteresis prediction model based on theory and geometric scaling. *Raats, P.A.C., Smiles, D., Warrick, A.W. (eds.) Environmental Mechanics, Water, Mass and Engergy Transfer in the Biosphere* (2002).
37. Hilfer, R., Capillary pressure, hysteresis and residual saturation in porous media. *Physica A: Statistical Mechanics and its Applications* **359** (2006), 119–128.
38. Hilfer, R. & Steinle, R., Saturation overshoot and hysteresis for twophase flow in porous media. *The European Physical Journal Special Topics* **223** (2014), 2323–2338.
39. Hilpert, M., On uniqueness for evolution problems with hysteresis. In *Mathematical models for phase change problems (Óbidos, 1988)*, vol. 88 of *Internat. Ser. Numer. Math.* Birkhäuser, Basel, 1989, pp. 377–388. Zbl0701.35009 MR1038080
40. Hoffmann, K.-H., Kenmochi, N., Kubo, M. & Yamazaki, N., Optimal control problems for models of phase-field type with hysteresis of play operator. *Adv. Math. Sci. Appl.* **17** (2007), 305–336. Zbl1287.49005 MR2337381
41. Javadi, A. & Elkassas, A., Numerical modeling of hydraulic hysteresis in unsaturated soils. *Transp. Porous Media* **85** (2010), 521–540. MR2737551
42. Jaynes, D., Comparison of soil-water hysteresis models. *J. Hydrol* **75** (1984).
43. Joekar-Niasar, V., Hassanizadeh, S. & Dahle, H., Non-equilibrium effects in capillarity and interfacial area in two-phase flow: dynamic pore-network modelling. *Journal of Fluid Mechanics* **655** (7 2010), 38–71. Zbl1197.76133 MR2660178
44. Johannesson, B. & Nyman, U., A numerical approach for non-linear moisture flow in porous materials with account to sorption hysteresis. *Transp. Porous Media* **84** (2010), 735–754. MR2721277
45. Kenmochi, N. & Visintin, A., Asymptotic stability for nonlinear PDEs with hysteresis. *European J. Appl. Math.* **5** (1994), 39–56. Zbl0805.35063 MR1270787
46. Koch, J., Rätz, A. & Schweizer, B., Two-phase flow equations with a dynamic capillary pressure. *European J. Appl. Math.* **24** (2013), 49–75. Zbl1261.76052 MR3041703
47. Kool, J. & Parker, J., Development and evaluation of closed-form expressions for hysteretic soil hydraulic properties. *Water Resour. Res.* **23** (1987).

48. Krasnosel′skiĭ, M., Darinskiĭ, B., Emelin, I.,, Zabreĭko, P., Lifšic, E. & Pokrovskiĭ, A. An operator-hysterant. *Dokl. Akad. Nauk SSSR* **190** (1970), 34–37. MR0257831
49. Krasnosel′skiĭ, M. & Pokrovskiĭ, A., *Systems with hysteresis*. Springer-Verlag, Berlin, 1989. Translated from the Russian by Marek Niezgódka. Zbl0665.47038 MR0987431
50. Krejčí, P., A monotonicity method for solving hyperbolic problems with hysteresis. *Apl. Mat.* **33** (1988), 197–203. Zbl0668.35065 MR0944783
51. Krejčí, P., *Hysteresis, convexity and dissipation in hyperbolic equations*. GAKUTO International Series. Mathematical Sciences and Applications, 8. Gakkōtosho Co., Ltd., Tokyo, 1996. Zbl1010.34038 MR1800964
52. Krejčí, P., Resonance in Preisach systems. *Appl. Math.* **45** (2000), 439–468.
53. Krejčí, P. & Petrov, A., Elasto-plastic contact problems with heat exchange. *Nonlinear Anal. Real World Appl.* **22** (2015), 551–567. Zbl1326.74042 MR3280851
54. Krejči, P., Sprekels, J. & Zheng, S., Asymptotic behaviour for a phase-field system with hysteresis. *J. Differential Equations* **175** (2001), 88–107. Zbl1021.35131 MR1849225
55. Lamacz, A., Rätz, A. & Schweizer, B., A well-posed hysteresis model for flows in porous media and applications to fingering effects. *Adv. Math. Sci. Appl.* **21** (2011), 33–64. Zbl1258.76155 MR2883874
56. Marchesin, D., Medeiros, H. & Paes-Leme, P., A model for two phase flow with hysteresis. In *Nonstrictly hyperbolic conservation laws (Anaheim, Calif., 1985)*, vol. 60 of *Contemp. Math.* Amer. Math. Soc., Providence, RI, 1987, pp. 89–107. Zbl0625.76100 MR0873534
57. Mayergoyz, I. D., *Mathematical models of hysteresis*. Springer-Verlag, New York, 1991. Zbl0723.73003 MR1083150
58. Mielke, A., Evolution of rate-independent systems. In *Evolutionary equations. Vol. II*, Handb. Differ. Equ. Elsevier/North-Holland, Amsterdam, 2005, pp. 461–559. Zbl1120.47062 MR2182832
59. Mielke, A. & Roubíček, T., *Rate-independent systems*, vol. 193 of *Applied Mathematical Sciences*. Springer, New York, 2015. Theory and application. Zbl1339.35006 MR3380972
60. Mualem, Y., Modified approach to capillary hysteresis based on a similarity hypothesis. *Water Resour. Res.* **9(5)** (1973).
61. Mualem, Y., A conceptual model of hysteresis. *Water Resour. Res* **10** (1974).
62. Mualem, Y., A modified dependent-domain theory of hysteresis. *Soil Sci.* **137(5)** (1984).
63. Mualem, Y. & Dagan, G., A dependent domain model of capillary hysteresis. *Water Resour. Res.* **11(3)** (1975).
64. Nieber, J., Bauters, T., Steenhuis, T. & Parlange, J.-Y., Numerical simulation of experimental gravity-driven unstable flow in water repellent sand. *Elsevier Journal of Hydrology* **231–232** (2000), 295–307.
65. Nieber, J., Dautov, R., Egorov, A. & Sheshukov, A., Dynamic capillary pressure mechanism for instability in gravity-driven flows; review and extension to very dry conditions. *Transp Porous Med* **58** (2005), 147–172. MR2129438
66. Otto, F., L^1-contraction and uniqueness for unstationary saturated-unsaturated porous media flow. *Adv. Math. Sci. Appl.* **7** (1997), 537–553. Zbl0888.35085 MR1476263
67. Parlange, J.-Y., Capillary hysteresis and the relationship between drying and wetting curves. *Water Resour. Res.* **12** (1976).
68. Pedroso, D., A solution to transient seepage in unsaturated porous media. *Comput. Methods Appl. Mech. Engrg.* **285** (2015), 791–816. MR3312687
69. Peszyńska, M. & Showalter, R., A transport model with adsorption hysteresis. *Differential Integral Equations* **11** 2 (1998), 327–340. Zbl1004.35033 MR1741849
70. Pham, H., Fredlund, D. & Barbour, S., A study of hysteresis models for soil-water characteristic curves. *Canadian Geotechnical Journal* **42** (2005), 1548–1568.
71. Philip, J., Similarity hypothesis for capillary hysteresis in porous materials. *J. Geophys. Res.* **69** (1964).

72. Philip, J., Horizontal redistribution with capillary hysteresis. *Water Resour. Res.* **27** (1991).
73. Plohr, B., Marchesin, D., Bedrikovetsky, P. & Krause, P., Modeling hysteresis in porous media flow via relaxation. *Computational Geosciences* **5** (2001), 225–256. Zbl1007.76081 MR1881940
74. Pop, I., Van Duijn, C., Niessner, J. & Hassanizadeh, S., Horizontal redistribution of fluids in a porous medium: The role of interfacial area in modeling hysteresis. *Advances in water resources* **32** (2009), 383–390.
75. Poulovassillis, A., Hysteresis of pore water, an application of the concept of independent domains. *Soil Sci.* **93** (1962).
76. Poulovassillis, A. & Kargas, G., A note on calculating hysteretic behavior. *Soil Sci. Soc. Am. J.* **64** (2000).
77. Preisach, F., Über die magnetische Nachwirkung. *Zeitschrift für Physik* **94** (1935), 277–302.
78. Rätz, A. & Schweizer, B., Hysteresis models and gravity fingering in porous media. *ZAMM Z. Angew. Math. Mech.* **94** (2014), 645–654. Zbl1297.76168 MR3230274
79. Richards, L., Capillary conduction of liquids through porous mediums. *Journal of Applied Physics* **1** (1931), 318–333.
80. Sander, G., Glidewell, O. & Norbury, J., Dynamic capillary pressure, hysteresis and gravity-driven fingering in porous media. *Journal of Physics Conference Series* **138** (2008), 1–14.
81. Schweizer, B., A stochastic model for fronts in porous media. *Ann. Mat. Pura Appl. (4)* **184** (2005), 375–393. Zbl1098.76068 MR2164264
82. Schweizer, B., Averaging of flows with capillary hysteresis in stochastic porous media. *European J. Appl. Math.* **18** (2007), 389–415. Zbl1118.76066 MR2331319
83. Schweizer, B., Homogenization of degenerate two-phase flow equations with oil trapping. *SIAM J. Math. Anal.* **39** 6(2008), 1740–1763. Zbl1172.35320 MR2390312
84. Schweizer, B., Instability of gravity wetting fronts for Richards equations with hysteresis. *Interfaces Free Bound.* **14** (2012), 37–64. Zbl1242.76323 MR2929125
85. Schweizer, B., The Richards equation with hysteresis and degenerate capillary pressure. *J. Differential Equations* **252** (2012), 5594–5612. Zbl1332.76061 MR2902128
86. Schweizer, B., *Partielle Differentialgleichungen. Eine anwendungsorientierte Einführung.* Heidelberg: Springer Spektrum, 2013. Zbl1284.35001
87. Scott, P., Farquhar, G. & Kouwen, N., Hysteretic effects on net infiltration. *Advances in infiltration* (1983).
88. Selker, J., Parlange, J.-Y. & Steenhuis, T., Fingered flow in two dimensions. Part 2. Predicting finger moisture profile. *Wat. Resources Res.* **28** (1992), 2523–2528.
89. Topp, G., Soil-water hysteresis: The domain theory extended to pore interaction conditions. *Soil Sci. Soc. Amer. Proc.* 35 (1971), 219–225.
90. Topp, G. & Miller, E., Hysteretic moisture characteristics and hydraulic conductivities for glass-bead media. *Soil Sci. Soc. Am. Proc.* 30 (1966), 156–162.
91. van Duijn, C., Eichel, H., Helmig, R. & Pop, I., Effective equations for two-phase flow in porous media: The effect of trapping on the microscale. *Transp. Porous Media* **69** (2007), 411–428. MR2328802
92. Van Duijn, C., Fan, Y., Peletier, L. & Pop, I., Travelling wave solutions for degenerate pseudo-parabolic equations modelling two-phase flow in porous media. *Nonlinear Analysis: Real World Applications* **14** 3 (2013), 1361–1383. Zbl1261.35125 MR3004506
93. Vázquez, J., *The porous medium equation.* Oxford Mathematical Monographs. The Clarendon Press Oxford University Press, Oxford, 2007.
94. Verdi, C. & Visintin, A., Numerical approximation of the Preisach model for hysteresis. *RAIRO Modél. Math. Anal. Numér.* **23** (1989), 335–356. Zbl0672.65115 MR1001333
95. Visintin, A., A model for hysteresis of distributed systems. *Ann. Mat. Pura Appl. (4)* **131** (1982), 203–231. Zbl0494.35052 MR0681564

96. Visintin, A., A phase transition problem with delay. *Control Cybernet.* **11** (1982), 5–18. Zbl0522.35089 MR0707337
97. Visintin, A., On the Preisach model for hysteresis. *Nonlinear Anal.* **8** (1984), 977–996. Zbl0977.35072 MR0760191
98. Visintin, A., *Differential models of hysteresis*, vol. 111 of *Applied Mathematical Sciences*. Springer-Verlag, Berlin, 1994. Zbl0820.35004 MR1329094
99. Visintin, A., *Models of phase transitions*. Progress in Nonlinear Differential Equations and their Applications, 28. Birkhäuser Boston Inc., Boston, MA, 1996.
100. Visintin, A., Quasilinear hyperbolic equations with hysteresis. *Ann. Inst. H. Poincaré Anal. Non Linéaire* **19** 4 (2002), 451–476. Zbl1027.35076 MR1912263
101. Visintin, A., Maxwell's equations with vector hysteresis. *Arch. Ration. Mech. Anal.* **175** (2005), 1–37. Zbl1145.78003 MR2106256
102. Visintin, A., Mathematical models of hysteresis. In *The Science of Hysteresis*, G. Bertotti & I. Mayergoyz, Eds. Elsevier, 2006, ch. 1, pp. 1–123. Zbl1149.35077
103. Visintin, A., P.D.E.s with hysteresis 30 years later. *Discrete Contin. Dyn. Syst. Ser. S* **8** (2015), 793–816. Zbl1304.35357 MR3356462
104. Weiss, P. & de Freudenreich, J., Etude de l'aimantation initiale en fonction de la température (suite et fin). *Arch. Sci. Phys. Nat.* **42** (1916).
105. Xiong, Y., Flow of water in porous media with saturation overshoot: A review. *Journal of Hydrology* **510** (2014), 353–362.